DOI: 10.1002/chem.200501230

Mechanistic Investigations of Imine Hydrogenation Catalyzed by Cationic Iridium Complexes

Marta Martín, Eduardo Sola,* Santiago Tejero, José L. Andrés, and Luis A. Oro*[a]

Abstract: Complexes $[IrH_2(\eta^6\text{-}C_6H_6)(P\mathit{i}Pr_3)]BF_4$ (**1**) and $[IrH_2(NCMe)_3(P\mathit{i}Pr_3)]BF_4$ (**2**) are catalyst precursors for homogeneous hydrogenation of *N*-benzylideneaniline under mild conditions. Precursor **1** generates the resting state $[IrH_2\{\eta^5\text{-}(C_6H_5)NHCH_2Ph\}(P\mathit{i}Pr_3)]BF_4$ (**3**), while **2** gives rise to a mixture of $[IrH\{PhN{=}CH(C_6H_4)\text{-}\kappa N,C\}(NCMe)_2(P\mathit{i}Pr_3)]BF_4$ (**4**) and $[IrH\{PhN{=}CH(C_6H_4)\text{-}\kappa N,C\}(NCMe)(NH_2Ph)(P\mathit{i}Pr_3)]BF_4$ (**5**), in which the aniline ligand is derived from hydrolysis of the imine. The less hindered benzophenone imine forms the catalytically inactive, doubly cyclometalated compound $[Ir\{HN{=}CPh(C_6H_4)\text{-}\kappa N,C\}_2(NH_2CHPh_2)(P\mathit{i}Pr_3)]BF_4$ (**6**). Hydrogenations with precursor **1** are fast and their reaction profiles are strongly dependent on solvent, concentrations, and temperature. Significant induction periods, minimized by addition of the amine hydrogenation product, are commonly observed. The catalytic rate law (THF) is rate $= k[\mathbf{1}][PhN{=}CHPh]p(H_2)$. The results of selected stoichiometric reactions of potential catalytic intermediates exclude participation of the cyclometalated compounds $[IrH\{PhN{=}CH(C_6H_4)\text{-}\kappa N,C\}(S)_2(P\mathit{i}Pr_3)]BF_4$ [S = acetonitrile (**4**), [D_6]acetone (**7**), [D_4]methanol (**8**)] in catalysis. Reactions between resting state **3** and D_2 reveal a selective sequence of deuterium incorporation into the complex which is accelerated by the amine product. Hydrogen bonding among the components of the catalytic reaction was examined by MP2 calculations on model compounds. The calculations allow formulation of an ionic, outer-sphere, bifunctional hydrogenation mechanism comprising 1) amine-assisted oxidative addition of H_2 to **3**, the result of which is equivalent to heterolytic splitting of dihydrogen, 2) replacement of a hydrogen-bonded amine by imine, and 3) simultaneous $H^{\delta+}/H^{\delta-}$ transfer to the imine substrate from the NH moiety of an arene-coordinated amine ligand and the metal, respectively.

Keywords: homogeneous catalysis · hydrogenation · imines · iridium · reaction mechanisms

Introduction

Homogeneous catalytic hydrogenation of C=N bonds is generally considered a difficult process and remains relatively underdeveloped and poorly understood when compared to that of C=C and C=O functionalities.[1] In spite of this, great industrial interest in imine hydrogenation has stimulated exhaustive empirical optimization of certain catalyst systems to reach activities and selectivities suitable for large-scale commercial application.[2]

The difficulties associated with hydrogenation of C=N bonds have been discussed in detail.[1a] Poisoning of the catalyst by hydrogenation products or hydrolysis byproducts (amines) is the most serious drawback for such reactions and greatly restricts the range of imines susceptible to homogeneous hydrogenation. In addition, characteristic features of the substrates, such as their reluctance to coordinate in an η^2-(C=N) mode and insert into metal–hydride bonds,[3,4] remain conceptual obstacles to achieving a mechanistic rationalization that could guide the systematic development of C=N hydrogenation catalysts. In this respect, however, the recently emerged concept of ionic hydrogenation is likely to play a decisive role.[5] Indeed, in contrast to pioneering mechanistic rationalizations featuring concerted C=N hydrogenation mechanisms extrapolated from those

[a] Dr. M. Martín, Dr. E. Sola, S. Tejero, Dr. J. L. Andrés, Prof. L. A. Oro
Departamento de Compuestos de Coordinación y Catálisis Homogénea
Instituto de Ciencia de Materiales de Aragón
Universidad de Zaragoza-CSIC and
Instituto Universitario de Catálisis Homogénea
Universidad de Zaragoza, 50009 Zaragoza (Spain)
Fax: (+34) 976-761-187
E-mail: sola@unizar.es
oro@unizar.es

Supporting information for this article is available on the WWW under http://www.chemeurj.org/ or from the author.

typical of alkene substrates,[1a,6] most of the recent results and discussions coincide in mechanistic proposals of the ionic type,[7] similar or related to those recognized in C=O hydrogenation.[5,8] These ionic mechanisms operate through elementary steps of proton and hydride transfer[9] and do not require the coordination of the hydrogen-accepting substrate to the catalyst metal center. Often, the feasibility of such mechanisms relies on the presence in the catalysts of ancillary ligands bearing acidic OH or NH groups, which facilitate proton transfer to the substrate.

In line with the aforementioned most recent proposals, the present study concludes that the mechanism of *N*-benzylideneaniline hydrogenation with the cationic catalyst precursor $[IrH_2(\eta^6\text{-}C_6H_6)(P\mathit{i}Pr_3)]BF_4$ (**1**) involves simultaneous transfer of proton and hydride from the catalyst to the imine. A distinctive feature of this system is that protons are transferred to the substrate from the NH moiety of a coordinated molecule of the amine hydrogenation product, so that ancillary ligands bearing NH groups are not required. This paper is followed by another describing a related mechanistic investigation on catalysis of C=N hydrogenation by the dinuclear complex $[Ir_2(\mu\text{-}H)(\mu\text{-}Pz)_2H_3(NCMe)(P\mathit{i}Pr_3)_2]$.[10] This second study also concludes a mechanism involving proton and hydride transfer from the catalyst to the imine, although in this case such elementary processes are consecutive rather than simultaneous, and the proton source is an acidic η^2-H_2 ligand instead of the coordinated amine product. Together, these conclusions may contribute to assessing the effectiveness of ionic imine hydrogenation and illustrate different alternative pathways compatible with this type of mechanism.

Results and Discussion

We reported that cationic dihydride iridium complexes of the type $[IrH_2(S)_3(P\mathit{i}Pr_3)]BF_4$ ($(S)_3 = \eta^6$-arene or $(NCMe)_3$) are effective catalyst precursors for C=C and C≡C hydrogenation.[11] These labile compounds were also recognized as suitable for the spectroscopic observation of reactive species formed under hydrogenation conditions, which facilitates the mechanistic interpretation of their catalysis. This capability, together with their previously recognized activity in catalytic C=N hydrogenation,[12] stimulated the present mechanistic study. Complexes $[IrH_2(\eta^6\text{-}C_6H_6)(P\mathit{i}Pr_3)]BF_4$ (**1**) and $[IrH_2(NCMe)_3(P\mathit{i}Pr_3)]BF_4$ (**2**) were chosen as catalyst precursors for the hydrogenation of *N*-benzylideneaniline (PhN=CHPh), an imine typically involved in catalyst development studies due to its resemblance to industrially interesting N-aryl-substituted imines, its moderate resistance to hydrolysis, and its relatively hindered nitrogen atom, which minimizes possible catalyst poisoning by the amine.

Catalyst resting states: Compounds **1** and **2** are closely related, and **2** can be readily obtained from **1** by substitution of the benzene ligand with an excess of acetonitrile. Accordingly, both compounds were found to catalyze the homogeneous hydrogenation of *N*-benzylideneaniline under mild conditions, although at noticeably different reaction rates (Figure 1).

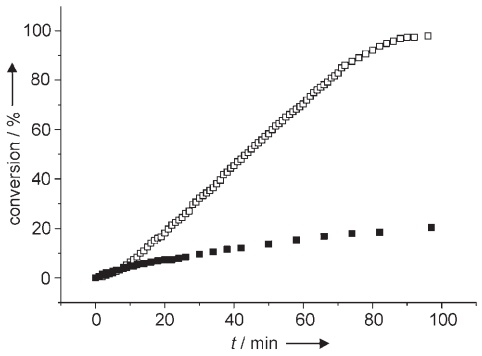

Figure 1. Hydrogenation of *N*-benzylideneaniline catalyzed by **1** (□) and **2** (■). Conditions: 1,2-dichloroethane (8 mL), $T = 333$ K, $p = 1.1$ bar, $[PhN{=}CHPh]_0 = 0.1\ mol\,L^{-1}$, $[catalyst] = 1.0 \times 10^{-3}\ mol\,L^{-1}$.

A possible explanation for this difference was straightforwardly inferred from the NMR spectra of these precursor complexes in $CDCl_3$ under conditions similar to those of catalysis, which evidence their transformation into different major species [Eq. (1)]. Thus, solutions obtained from **1** contained a sole observable iridium complex, namely, $[IrH_2\{\eta^5\text{-}(C_6H_5)NHCH_2Ph\}(P\mathit{i}Pr_3)]BF_4$ (**3**), in which the hydrogenation product is coordinated to the metal center through a phenyl ring. In contrast, precursor **2** generated a mixture of $[IrH\{PhN{=}CH(C_6H_4)\text{-}\kappa N,C\}(NCMe)_2(P\mathit{i}Pr_3)]BF_4$ (**4**) and $[IrH\{PhN{=}CH(C_6H_4)\text{-}\kappa N,C\}(NCMe)(NH_2Ph)(P\mathit{i}Pr_3)]BF_4$ (**5**), both of which contain a cyclometalated molecule of the substrate as ligand.

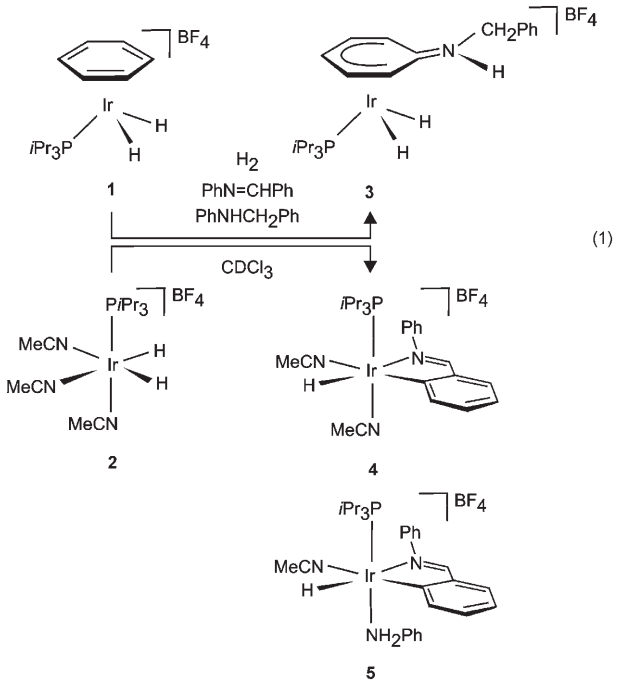

(1)

The aniline ligand of complex **5** is likely the result of partial imine hydrolysis due to adventitious water,[13] and accordingly **5** virtually disappeared from the catalysis solutions when carefully dried substrates and solvents were used. In any case, the presence of up to 5 equiv of aniline per equivalent of catalyst was found to be irrelevant for the catalytic activity of **2**. Moreover, the same reaction profile has been obtained with any of the complexes **2, 4**, or **5** as catalyst precursor.

Catalyst resting states **3**–**5** were independently prepared and fully characterized. Figure 2 shows the X-ray structures of complex **3** and the cation of **5**, and Table 1 lists selected bond lengths and and angles.

Table 1. Selected bond lengths [Å] and angles [°] for **3** and **5**.

3		**5**	
Ir–P	2.2553(17)	Ir–P	2.2688(9)
Ir–C(1)	2.500(6)	Ir–N(1)	2.221(3)
Ir–C(2)	2.274(6)	Ir–N(2)	2.085(3)
Ir–C(3)	2.245(6)	Ir–N(3)	2.183(3)
Ir–C(4)	2.282(7)	Ir–C(3)	2.000(3)
Ir–C(5)	2.258(7)		
Ir–C(6)	2.348(6)		
N–C(1)	1.335(9)	N(1)–C(1)	1.287(4)
N–C(7)	1.466(9)	N(1)–C(8)	1.432(4)
C(1)–C(2)	1.455(10)	N(2)–C(14)	1.135(4)
C(1)–C(6)	1.419(9)	N(3)–C(16)	1.446(4)
C(2)–C(3)	1.393(9)	C(1)–C(2)	1.438(5)
C(3)–C(4)	1.402(10)	C(14)–C(15)	1.456(5)
C(4)–C(5)	1.401(10)		
C(5)–C(6)	1.399(9)		
C(7)–C(8)	1.506(10)		
H(1)···F(1)	2.55(9)		
H(1)···F(2)	2.00(9)	N(1)-Ir-C(3)	78.80(12)
C(1)-N-C(7)	124.0(6)	N(2)-Ir-C(3)	174.94(12)
C(8)-C(7)-N	114.5(6)	P-Ir-N(3)	172.98(8)

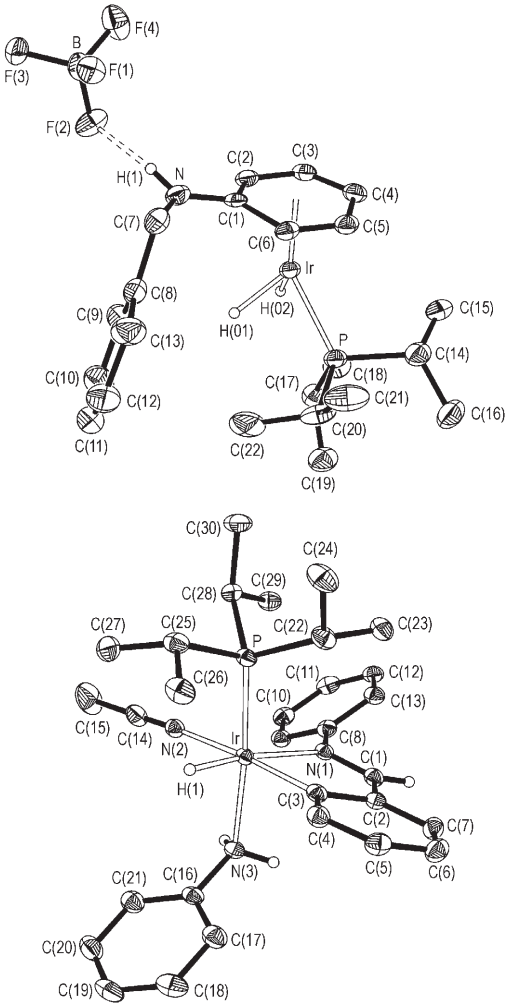

Figure 2. Molecular structures of **3** (top) and the cation of **5** (bottom).

Compound **3** can be readily obtained from **1** after substitution of the benzene ligand by *N*-benzylaniline in weakly coordinating solvents such as acetone. Alternatively, the complex can also be obtained by the general synthetic procedure previously described for this type of Ir^{III} arene dihydrides.[12] The compound crystallizes as an ion pair[14] with a short H(1)–F(2) distance of 2.00(9) Å. This weak interaction is retained in $CDCl_3$ and CD_2Cl_2 solutions, as evidenced by the similar diffusion coefficients found for anion and cation in NMR pulsed gradient spin echo experiments and a cross-peak in the ^1H,^{19}F HOESY spectrum, but not in more polar solvents such as [D_4]methanol (see Supporting Information). Another significant structural feature of **3** is the arene coordination. Five of the six Ir–C distances, Ir–C(2) to Ir–C(6), are within the range of 2.24–2.35 Å found in the η^6-mesitylene analogue of **3**,[11a] whereas the Ir–C(1) distance is clearly longer (2.500(6) Å). This is consistent with the short N–C(1) distance of 1.335(9) Å, which suggests the amine is better described as an η^5 ligand with a C=N bond. The variable-temperature ^1H NMR spectra of the compound (Figure 3) agree with such a bonding description by revealing hindered rotation around the proposed C=N bond at low temperature. The rates of rotation were obtained by line-shape analysis of the ^1H NMR spectra at various temperatures (Supporting Information), and the activation parameters were estimated as $\Delta H^{\neq} = 12.2 \pm 0.5$ kcal mol^{-1} and $\Delta S^{\neq} = 0 \pm 1$ cal mol^{-1} K^{-1}. An Rh^I compound related to **3**, with an η^4-coordinated *N*-benzylaniline ligand, was characterized during a study on *N*-benzylideneaniline hydrogenation catalyzed by [$RhH_2(PPh_3)_2$(methanol)$_2$]PF_6 and reported to be catalytically inactive.[15]

Compound **4** was prepared by reaction of **2** with *N*-benzylideneaniline, a process that also produces H_2. Related complex **5** was conveniently obtained by addition of water to the above reaction or after treatment of **4** with 1 equiv of aniline. Complexes **4** and **5** show similar ^1H and $^{13}C\{^1H\}$ NMR spectra, both indicative of the presence of cyclometalated imine ligands. A characteristic signal in the ^1H spectrum is a hydride resonance at $\delta = -20$ (dd, J(H,P) = 23 Hz) with a small J(H,H) coupling of about 1 Hz with the N=CH proton. The cyclometalated ligands also give rise to characteristic doublets in the $^{13}C\{^1H\}$ NMR spectrum (J(C,P)

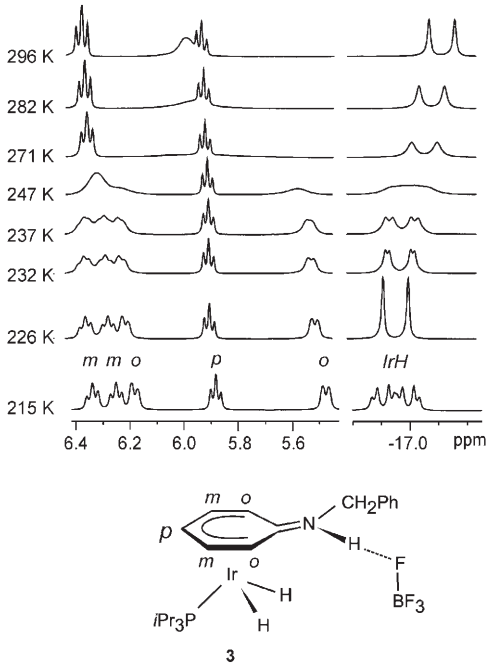

Figure 3. Aromatic and hydride regions of the variable-temperature ^{1}H NMR spectrum of **3** in CD_2Cl_2.

≈8 Hz), attributable to the aromatic carbon atom bonded to the metal center. The presence of a cyclometalated imine ligand was corroborated by the X-ray structure of **5** (Figure 2). Such activation and coordination of aryl imines is common for transition metal complexes,[16] and closely related rhodium and iridium complexes have been reported.[17]

The different resting states formed from **1** and **2** under otherwise the same reaction conditions suggest that the presence or absence in the reaction of potentially good ligands (e.g., acetonitrile) determines the major species present during hydrogenation and hence catalyst performance. Accordingly, the use of more strongly coordinating aryl imines as substrates favors cyclometalation irrespective of the catalyst precursor, as illustrated in Equation (2) for benzophenone imine. Under the conditions of a catalytic reaction, this imine quantitatively afforded the doubly cyclometalated species $[Ir\{HN{=}CPh(C_6H_4)\text{-}\kappa N,C\}_2(NH_2CHPh_2)(P\mathit{i}Pr_3)]BF_4$ (**6**), which also contains a *N*-coordinated molecule of the hydrogenation product (Figure 4, Table 2). This compound is catalytically inactive; thus, besides amine coordination, multiple substrate cyclometalation can eventually result in catalyst deactivation.

Table 2. Selected bond lengths [Å] and angles [°] for **6**.

Ir–P	2.304(2)	P-Ir-N(1)	174.33(19)
Ir–N(1)	2.131(7)	N(2)-Ir-C(22)	77.7(3)
Ir–N(2)	2.103(6)	N(2)-Ir-C(35)	167.4(3)
Ir–N(3)	2.084(7)	N(3)-Ir-C(22)	176.3(3)
Ir–C(22)	2.015(8)	N(3)-Ir-C(35)	77.8(3)
Ir–C(35)	2.063(8)		
N(1)–C(1)	1.515(9)		
N(2)–C(14)	1.312(9)		
N(3)–C(27)	1.284(9)		

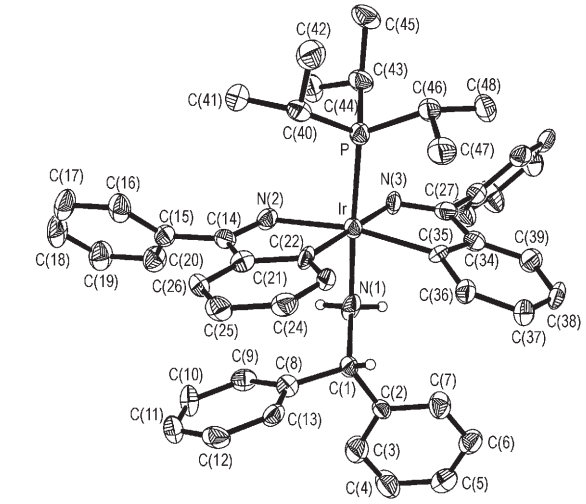

Figure 4. Molecular structure of the cation of **6**.

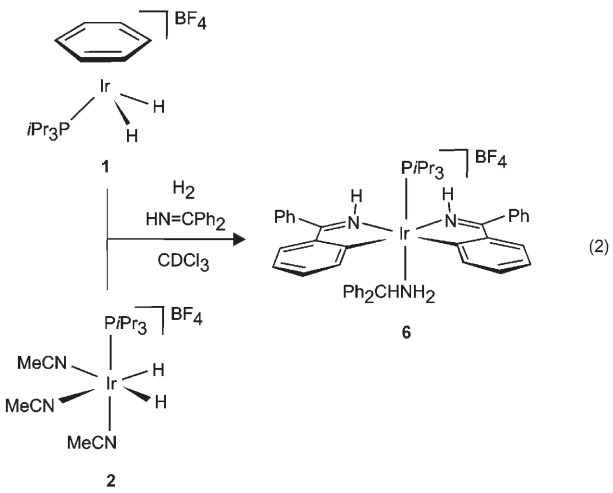

Weakly coordinating solvents such as acetone and methanol also favor *N*-benzylideneaniline cyclometalation, although the resulting cyclometalated products are disfavored relative to complex **3** under hydrogenation conditions [Eq. (3)]. Treatment of **1** with *N*-benzylideneaniline in $[D_6]$acetone or $[D_4]$methanol readily afforded $[IrH\{PhN{=}CH(C_6H_4)\text{-}\kappa N,C\}(S)_2(P\mathit{i}Pr_3)]BF_4$ [S = $[D_6]$acetone (**7**) or $[D_4]$methanol (**8**)]. The dihydrogen evolved in these reactions partially hydrogenates the imine reactant, even under a stream of argon. Although such a process did not preclude nearly quantitative generation of **7** and **8** in their respective solvents, our attempts to isolate the compounds as solids systematically afforded oily residues, even in the presence of noncoordinating anions other than BF_4^-. Nevertheless, these solvent complexes could be conveniently characterized in solution by NMR spectroscopy: their ^{1}H and $^{13}C\{^1H\}$ NMR spectra closely resemble those of the parent acetonitrile

complexes **4** and **5**. The [D_4]methanol complex **8** undergoes slow deuteration of the hydride ligand. The deuterated isotopomer displays a characteristic downfield isotopic shift of 0.07 ppm in the $^{31}P\{^1H\}$ NMR signal.[11,18]

Exposure of the aforementioned solutions containing **7** or

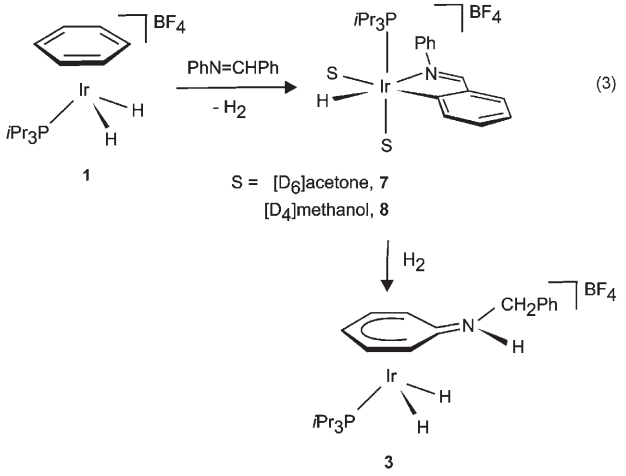

8 to dihydrogen atmosphere was observed by NMR spectroscopy to result in transformation of the cyclometalated compounds into complex **3** [Eq. (3)]. In the absence of excess amine, the previously reported tris-acetone complex $[IrH_2([D_6]acetone)_3(PiPr_3)]BF_4$ (**9**)[11a] or its [D_4]methanol analogue $[IrH_2([D_4]methanol)_3(PiPr_3)]BF_4$ (**10**) was respectively detected in equilibrium with **3**. However, the excess amine present under catalytic conditions displaces these equilibria towards complex **3**, which is the only NMR-detectable metal complex in catalytic reactions in these solvents. Complex **3** was recognized (by NMR spectroscopy) to also be the sole catalyst resting state when precursor **1** is used in other solvents such as 1,2-dichloroethane or THF.

Solvents and induction periods: All solvents favoring formation of resting state **3** were found to favor fast *N*-benzylideneaniline hydrogenation. However, the observed reaction profiles are rather different for each solvent and also depend on concentration and temperature. Figure 5a shows H_2-uptake profiles typically obtained in 1,2-dichloroethane, THF, and acetone for reactions catalyzed by precursor **1**.

The reaction in 1,2-dichloroethane has a long induction period, which is suggestive of an autocatalytic process. A shorter induction period is observed in THF, in which the reaction is slower than in chlorinated solvents. The reaction in acetone is faster, and its profile corresponds well to that expected for a reaction with first-order dependence on imine concentration. Catalysis in methanol is faster than in all above-mentioned solvents and, under the conditions of Figure 5a, the observed reaction rate corresponds to that of dihydrogen diffusion into methanol. Lowering the catalyst concentration, as illustrated in Figure 5b, results in a seemingly exponential profile. Nevertheless, this figure also illustrates that, even in this solvent, a significant induction period appears when the reaction temperature is decreased.

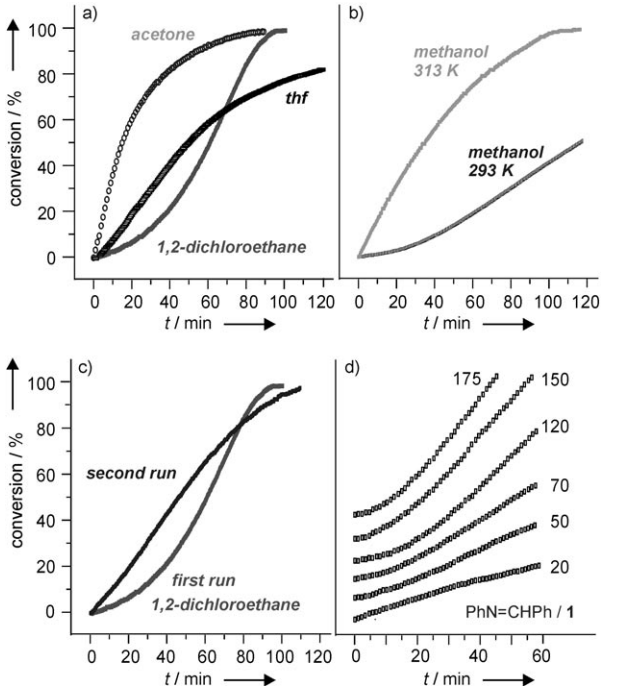

Figure 5. Experimental H_2-uptake profiles for the hydrogenation of *N*-benzylideneaniline catalyzed by **1**. Conditions: a) Solvent (8 mL), $T=313$ K, $p=1.1$ bar, $[PhN{=}CHPh]_0=0.1\ mol\,L^{-1}$ $[\mathbf{1}]=5.0\times10^{-3}\ mol\,L^{-1}$. b) Methanol (8 mL), $p=1.1$ bar, $[PhN{=}CHPh]_0=0.1\ mol\,L^{-1}$, $[\mathbf{1}]=7.66\times10^{-4}\ mol\,L^{-1}$. c) 1,2-Dichloroethane (8 mL), $T=313$ K, $p=1.1$ bar, $[PhN{=}CHPh]_0=0.1\ mol\,L^{-1}$, $[\mathbf{1}]=5.0\times10^{-3}\ mol\,L^{-1}$. d) THF (8 mL), $T=313$ K, $p=1.0$ bar, $[\mathbf{1}]=1.25\times10^{-3}\ mol\,L^{-1}$.

Our investigation of possible origins of the observed induction periods initially focused on generation of resting state **3** from precursor **1**. However, the reaction profiles obtained with any of these complexes as catalyst precursor are similar. In this context, it is noteworthy that the commercial *N*-benzylideneaniline used in this study contains aniline as impurity (ca. 0.5% by GC), which can readily replace the labile benzene ligand of precursor **1** during the setup operation prior to catalysis to generate the aniline analogue of **3**.[12] Further studies revealed an apparent qualitative correlation between the length of the induction periods and the initial concentrations of imine substrate and amine product. Thus, addition of amine at the beginning of the catalytic reactions shortens the induction period. This is illustrated by the profiles in Figure 5c, which correspond to two consecutive reactions in 1,2-dichloroethane, the second of which was initiated in the presence of 0.8 mmol of amine product. Such an effect suggests that, besides its contribution to form resting state **3**, the amine product could play a significant role in the hydrogenation mechanism. The concentration of imine substrate also seems to influence the initial progress of the reaction, since its increase results in longer induction periods in THF (Figure 5d).

Kinetics: The dependence of the hydrogenation rate on the concentration of catalyst and substrates was investigated in reactions catalyzed by **1** at 313 K. Since the presence of ad-

ventitious water has been recognized as problem for the reproducibility of these hydrogenations, carefully dried THF was chosen as the solvent for this kinetic study. The reaction rates were determined by H_2-uptake measurements at constant pressure (see Experimental Section). To minimize the effect of the conditions-dependent activation periods, the complete reaction profiles, except the initial part, were adjusted to exponentially growing functions. Hence, the values of initial rates used in the kinetic analysis (Table 3) are those extrapolated from these fittings.

Table 3. Initial reaction rates for the hydrogenation of *N*-benzylideneaniline catalyzed by **1** in THF at 313 K.

[**1**] [mol L^{-1}]	[PhN=CHPh] [mol L^{-1}]	$p(H_2)$ [bar][a]	Initial rate [mol s^{-1}]
1.00×10^{-3}	1.00×10^{-1}	0.60	4.22×10^{-8}
1.25×10^{-3}	1.00×10^{-1}	0.60	6.61×10^{-8}
1.56×10^{-3}	1.00×10^{-1}	0.60	6.70×10^{-8}
1.87×10^{-3}	1.00×10^{-1}	0.60	9.17×10^{-8}
2.50×10^{-3}	1.00×10^{-1}	0.60	1.05×10^{-7}
1.25×10^{-3}	4.35×10^{-2}	0.60	2.95×10^{-8}
1.25×10^{-3}	5.24×10^{-2}	0.60	3.64×10^{-8}
1.25×10^{-3}	7.90×10^{-2}	0.60	5.20×10^{-8}
1.25×10^{-3}	1.60×10^{-1}	0.60	9.55×10^{-8}
1.25×10^{-3}	2.09×10^{-1}	0.60	1.24×10^{-7}
1.25×10^{-3}	2.30×10^{-1}	0.60	1.34×10^{-7}
1.25×10^{-3}	1.00×10^{-1}	1.00	1.09×10^{-7}
1.25×10^{-3}	1.00×10^{-1}	0.86	9.24×10^{-8}
1.25×10^{-3}	1.00×10^{-1}	0.40	5.05×10^{-8}

[a] THF vapor pressure at 313 K = 0.4 bar.

The Figure 6 shows logarithmic representations of these initial rates as a function of initial precursor and substrate concentrations and dihydrogen partial pressure. The least-squares fits in these plots indicate first-order dependence of the reaction rate on catalyst, imine, and dihydrogen concentrations. Unfortunately, these results are little informative about the possible rate-determining step of the process, since they are compatible with various sequences of elementary reactions.

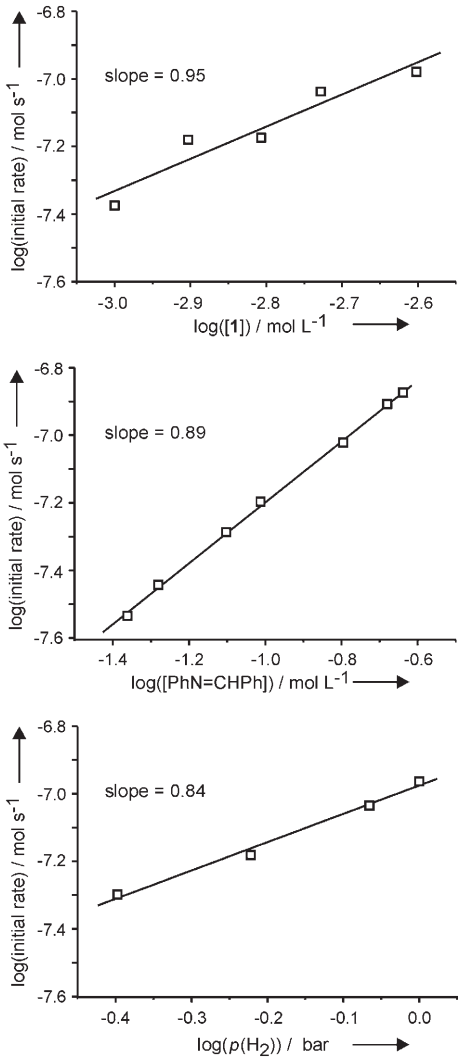

Figure 6. Logarithmic plots for the dependence of the initial hydrogenation rates on concentration of precursor **1** (top), initial *N*-benzylideneaniline concentration (center), and dihydrogen pressure (bottom).

Reactivity studies: The aforementioned chemistry of complexes **1** and **2** revealed two types of compound compatible with the catalytic conditions, the reactivity of which may be significant in the context of hydrogenation: arene complex **3** and the solvent complexes $[IrH\{PhN{=}CH(C_6H_4)\text{-}\kappa N,C\}(S)_2(P\mathit{i}Pr_3)]BF_4$ [S = acetonitrile (**4**), [D$_6$]acetone (**7**), [D$_4$]methanol (**8**)].

The solvent complexes were not detected by NMR spectroscopy in the fastest catalytic reactions, although their presence as traces cannot be ruled out. In principle, these compounds have several features highly desirable for a catalyst candidate, such as two labile solvent ligands, a coordinated molecule of the imine substrate, and a demonstrated ability to activate dihydrogen [Eq. (3)]. Nevertheless, the participation of these compounds in hydrogenation cannot be straightforwardly deduced from the above-mentioned experiments, since their solutions always contain *N*-benzylaniline or aniline, which can readily form complex **3** or its aniline analogue under dihydrogen atmosphere. To determine whether solvent complexes **4, 7**, and **8** are involved in the hydrogenation pathway, their reactions with dihydrogen were studied by NMR spectroscopy in the presence of a soluble tetraphenylborate salt. This anion is an excellent arene ligand, capable of displacing other neutral arenes or solvent molecules from iridium(III) dihydrides to form the zwitterionic complex $[IrH_2\{(\eta^6\text{-}C_6H_5)BPh_3\}(P\mathit{i}Pr_3)]$ (**11**),[12] which is inactive in imine hydrogenation. In these experiments, it was expected that the BPh_4^- ligand would eliminate **3** from the solutions and thus avoid any subsequent evolution of the initial organic products of the reaction between dihydrogen and the solvent complexes. Indeed, the reactions [Eq. (4)] quantitatively afforded **11** together with amine/imine mixtures containing more than 90% of the imine. This result indicates that these solvent-coordinated cyclometalated imine complexes do not contribute to hydrogenation catalysis, a conclusion that agrees with observa-

tions made by James et al. for related rhodium bis-phosphine compounds.[17]

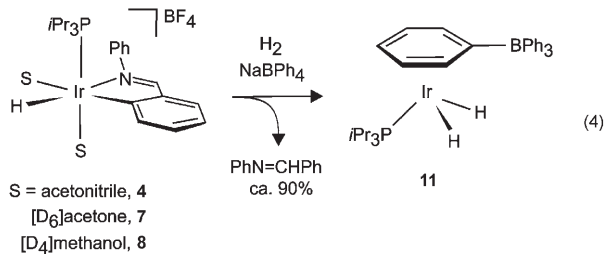

Reactions of resting state **3** with components of the catalytic reaction have been investigated by NMR methods. In the presence of excess *N*-benzylideneaniline, solutions of **3** in $[D_6]$acetone and $[D_4]$methanol afford the cyclometalated species **7** and **8**, respectively [Eq. (5)]. These reactions are likely mediated by tris-solvent complexes **9** and **10**, respectively, since in less strongly coordinating solvents such as THF or CD_2Cl_2 **3** remains unchanged under the same conditions. Nevertheless, the experiment in Equation (4) indicates that this reaction sequence is reversible in the presence of dihydrogen, and this suggests that the compounds in Equation (5) should be in equilibrium during catalysis. The NMR observations under catalytic conditions in these solvents show that such an equilibrium, nonproductive from the viewpoint of imine hydrogenation, is well displaced towards amine complex **3**.

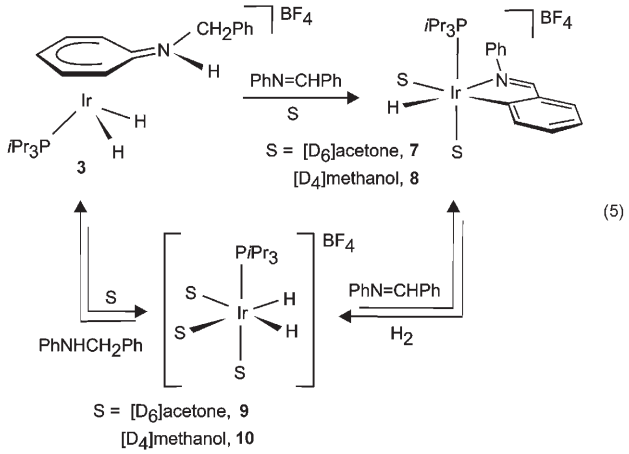

In chlorinated solvents, mixtures of **3** and imine substrate evolve into new reaction products after prolonged heating above 323 K. The new products were identified as the neutral dinuclear complexes $[Ir_2(\mu\text{-Cl})(\mu\text{-H})ClH\{PhN{=}CH(C_6H_4)\text{-}\kappa N,C\}_2(PiPr_3)_2]$ (**12**) and $[Ir_2(\mu\text{-Cl})(\mu\text{-H})Cl_2\{PhN{=}CH(C_6H_4)\text{-}\kappa N,C\}_2(PiPr_3)_2]$ (**13**) [Eq. (6)], which could conveniently be prepared and isolated from reactions between **1** and *N*-benzylideneaniline in chloroform. The $^{13}C\{^1H\}$ NMR spectra of the complexes show characteristic signals for the cyclometalated imine ligands, while the ^1H NMR spectra display high-field resonances attributable to bridging hydrides coordinated *trans* to one phosphine and *cis* to another. The FAB+ mass spectra also agree with the proposed dinuclear character of the compounds. The formation of these complexes likely involves thermally induced substitution of hydride by chloride, which is relatively common for iridium(III) hydrides in chlorinated solvents.[19] In any case, the evolution of such dinuclear compounds seems too slow to have any significance for catalytic imine hydrogenation. Furthermore, **12** and **13** are inactive as catalyst precursors in *N*-benzylideneaniline hydrogenation.

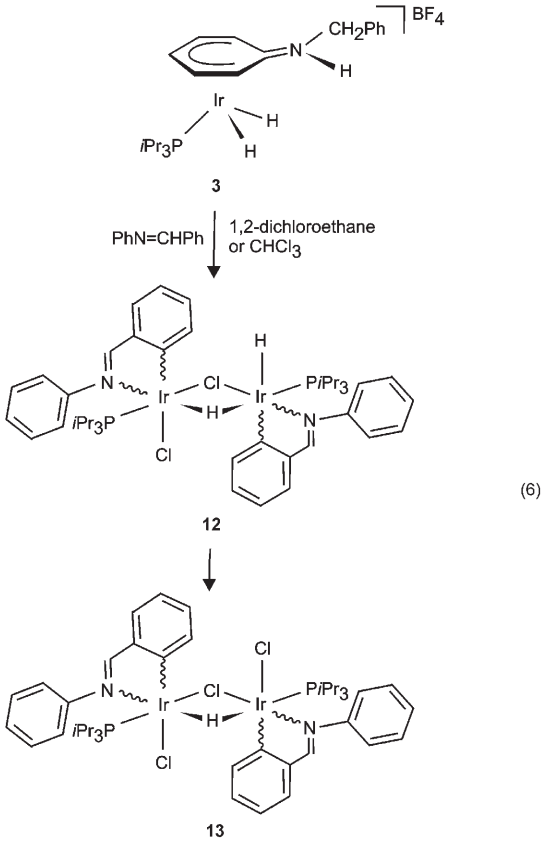

Complex **3** was observed not to form new products by reaction with dihydrogen, although the use of D_2 revealed a rich chemistry behind this apparent lack of activity. Exposure of CD_2Cl_2 solutions of **3** to D_2 atmosphere at room temperature resulted in slow incorporation of deuterium into the complex, which becomes detectable by NMR after about 1 h. of reaction [Eq. (7)]. Initially, H/D exchange selectively affords the isotopomer deuterated at the NH moiety of the arene ligand, as evidenced by both the disappearance of the ^1H NMR resonance due to the NH proton and the parallel transformation of the doublet corresponding to the neighboring CH_2 group into a singlet. Deuterium incorporation at the hydride positions becomes observable only after nearly complete deuteration of the NH group.

Each hydride deuteration provokes a small downfield isotopic shift of 0.034 ppm in the $^{31}P\{^1H\}$ NMR signal of **3**, similar in magnitude to those observed in related arene derivatives.[11a]

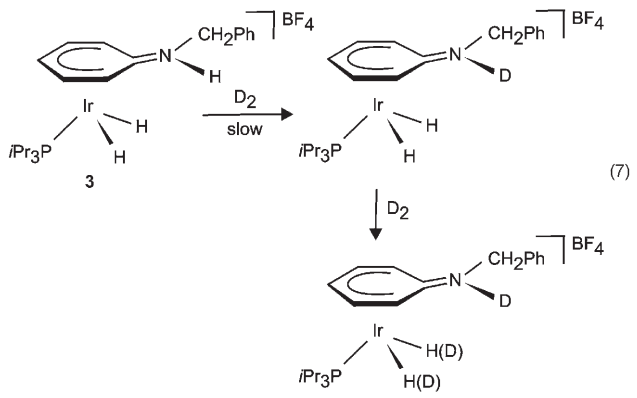

(7)

A possible mechanism for D_2 activation and H/D exchange in **3** is formation of a dihydrogen intermediate via an IrH···HN hydride–proton bond, as previously proposed to explain the heterolytic splitting of dihydrogen and intramolecular hydrogen exchange in related transition-metal complexes bearing pendant amino groups.[20] However, this option seems unlikely for complex **3** due to the long distance between the NH group and hydride ligands, and because such dihydrogen-mediated D_2 activation would preferably form dideuterated isotopomers of **3**, which are not observed in the initial stage of our reaction. On the other hand, assuming that D_2 activation occurs at the iridium center, any possible IrH/NH hydrogen-exchange mechanism would account for the observed deuteration selectivity, since the kinetic isotope effect associated with N–H bond cleavage is expected to be larger than that for Ir–H splitting, so that NH deuteration is thermodynamically preferred.[21]

Further insight into the possible mechanism of deuterium incorporation was obtained from the reaction of **3** with D_2 in the presence of added *N*-benzylaniline. The amine was found to render deuterium incorporation clearly observable after a few minutes of reaction. Furthermore, deuterium was observed to be preferentially incorporated into the free amine NH moiety, while the sequential deuteration of Equation (7) begins only after almost complete deuteration of this NH group. Such reaction acceleration and deuteration selectivity strongly suggest that the amine participates in both the dihydrogen activation process and IrH/NH scrambling.

These experimental observations also suggest that hydrogen bonding could be important for the development of catalytically active species from resting state **3**. Unfortunately, neither the interaction between **3** and *N*-benzylaniline suggested by the latter experiment nor other possible interactions between **3** and the imine substrate were directly observable by NMR or IR spectroscopy, or inferable from NMR diffusion experiments. Nevertheless, the expected participation of the NH group of **3** in hydrogen bonds can be corroborated by fast deuteration of this group in [D_4]methanol solution [Eq. (8)]. In a reaction also related to this behavior, strong bases such as NaH have been found to deprotonate **3** to give the neutral derivative [IrH_2-{η^5-(C_6H_5)NCH_2Ph}($PiPr_3$)] (**14**) [Eq. (8)], which is relatively unstable and could not be isolated, although it has been characterized by NMR spectroscopy in [D_8]THF solution. The NMR spectra of **14** indicate hindered rotation around the C=N bond at the highest attainable temperature, a likely consequence of the expected increase in bond order after deprotonation.

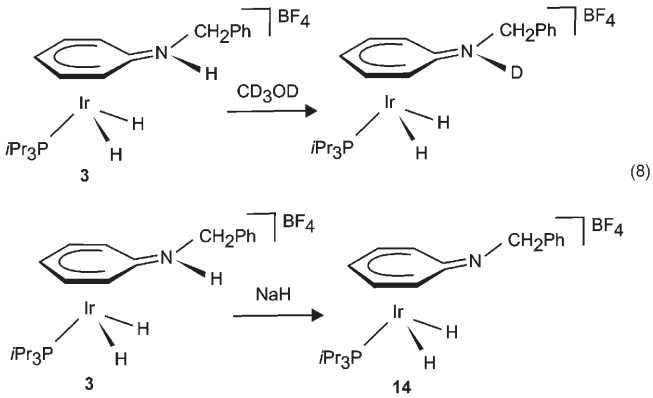

(8)

Calculations on model complexes: The experimentally elusive hydrogen-bonding chemistry of complex **3** has been examined in the model compound [IrH_2{η^5-(C_6H_5)$NHCH_3$}-(PH_3)]BF_4 (**3′**) at the MP2/basis-II level of theory. The optimized structure of this model complex reproduces well the structural parameters found in the X-ray structure of **3** (see Supporting Information).

Calculations on the cation of **3′** in the presence of models for the imine substrate and amine product ($HN{=}CH_2$ and H_2NCH_3, respectively) indicate that such molecules can form stable adducts similar to that experimentally found with the tetrafluoroborate anion, but also others featuring hydrogen bonds with the hydride ligands. Formation of adducts **15′** and **16′** (Figure 7) is exothermic by about 17 kcal mol^{-1}, a value much larger than the energies commonly associated with hydrogen bonding. This unusual stabilization might be qualitatively rationalized by long-range modifications induced by the hydrogen bonds, which affect the coordination mode of the arene ligand. For example, on formation of imine adduct **15′**, the N–C(*ipso*) distance of the arene ligand changes only slightly, from 1.35 to 1.33 Å, but the Ir–C(*ipso*) bond is elongated by 0.03 Å, while all other Ir–C distances shorten by about 0.005 Å; thus, the η^5 character of the arene ligand is enhanced. For these adducts, we explored the possible generation of catalytically active species by proton transfer from the NH moiety to the amine or the imine, as experimentally observed with strong bases. However, the large energy barriers found for such processes hardly seem compatible with the fast catalytic reactions.

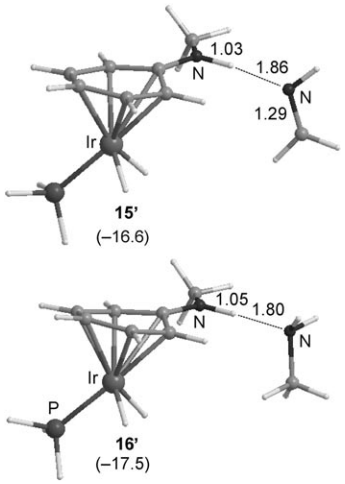

Figure 7. MP2/Basis-II optimized structures of hydrogen-bonded amine and imine adducts of model cation **3′**. Values in parentheses are electronic energies [kcal mol^{-1}] relative to the separate reactants (**3′** + HN=CH_2 + H_2NCH_3). Interatomic distances in Å.

On the contrary, a facile hydrogenation pathway was found to start from the less stable amine adduct **17′** (Figure 8), the behavior of which can itself explain various aforementioned experimental observations on the system. With regard to the Ir–H and N–H distances, this adduct could be formally described as an iridium(I) complex in which an ammonium moiety is connected to both the metal center and the nitrogen atom of the arene ligand through hydrogen bonds. The bridging position of the ammonium moiety between the metal center and the NH group is consistent with the experimentally inferred involvement of the amine in deuterium exchange between these two positions. Moreover, the "incomplete" deprotonation of the iridium center effected by the amine was found to render oxidative addition of dihydrogen to the formally Ir^{I} center a facile process, at the expense of a change in the coordination mode of the arene ligand from η^6 to η^4 (Figure 8).

After oxidative addition of dihydrogen, the Ir^{III} center again becomes coordinatively saturated, and hence metal deprotonation cannot be reversed, and alternative protonation of the arene ligand NH is favored. This entire complex process occurs simultaneously through the transition state **18TS** (Figure 8). The final result of this reaction is equivalent to the heterolytic splitting of dihydrogen by metal complexes bearing amido[8a,b,9,22] or sulfido groups,[23] which requires these groups to be directly bonded, or at least very close,[20] to the metal center. This condition is not fulfilled by our system, although the same practical result can be achieved with the help of amine by a mechanism formally different to that of heterolytic splitting.

The final product of dihydrogen oxidative addition, trihydride **19′** (Figure 8), is analogous to the imine species **21′**, the energy of which is just 3.6 kcal mol^{-1} higher. The transformation between these two analogues could take place by initial dissociation of the hydrogen-bonded amine from **19′**, or through an associative step involving an additional hydrogen bond between the incoming imine and the remaining NH proton. Considering that our model system could hardly afford a favorable estimation of the experimental, very crowded, associative route, we restricted our calculations to the feasibility of dissociative exchange through intermediate **20′**. This amine complex could undergo imine exchange prior to facile bifunctional hydrogenation of the imine that regenerates model cation **3′**. The early transition state of the latter process (**22TS**, Figure 8) is similar to those previously described for ionic C=O hydrogenation and transfer hydrogenation,[8] although it shows a larger degree of substrate protonation, as previously anticipated for C=N hydrogenation.[7c] Even though the two new N–H and C–H bonds simultaneously form in this step, the transition state features a rather asymmetric situation with an almost finished iminium cation (N–H 1.05 Å) and a very incipient C–H bond (C–H 1.83 Å). The NPA partial charges of the formal hydride and proton undergoing transfer of −0.16 and +0.44, respectively, also reflect the polar nature of this hydrogenation.

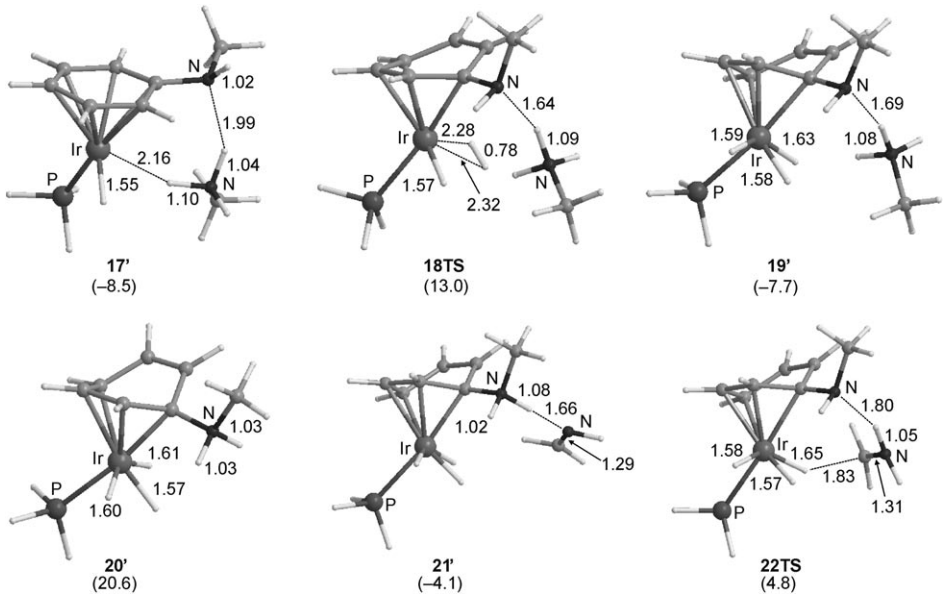

Figure 8. MP2/Basis-II optimized structures of intermediates and transition states involved in the model imine hydrogenation. Values in parentheses are electronic energies [kcal mol^{-1}] relative to the separate reactants (**3′** + HN=CH_2 + H_2NCH_3 + H_2). Interatomic distances in Å.

Mechanism: The above calculations allow the formulation of a mechanism for catalytic imine hydrogenation which strongly depends on the effectiveness of hydrogen bonding [Eq. (9)]. Reduction of C=N takes place in the outer coordination sphere of a catalyst formed "in situ" with participation of the N-aryl-substituted imine hydrogenation product. This characteristic confers on the system an apparent disadvantage with regard to other "designed" catalysts active in bifunctional hydrogenations of polar bonds, since the metal –nitrogen distance in the catalyst is too long to accomplish heterolytic splitting of the dihydrogen substrate. However, this inconvenience can be overcome by formal deprotonation of the metal atom by the amine product, which allows for a subsequent oxidative addition of dihydrogen that eventually forces the proton to migrate to the nitrogen atom. Such a process is feasible also due to the coordinative versatility of the arene ligand, which can change its coordination mode to η^4.

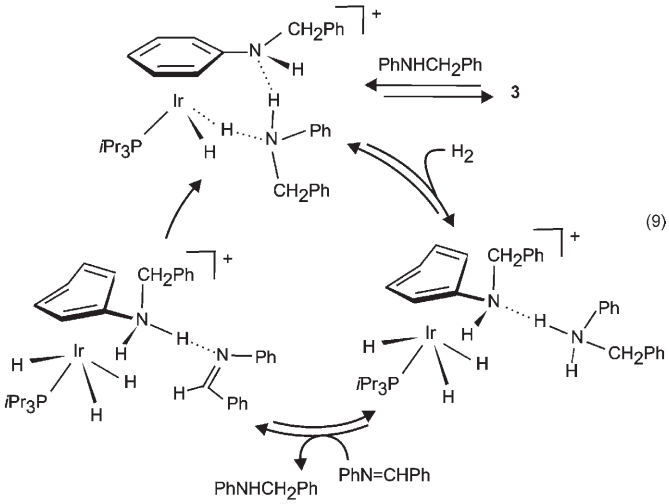

(9)

The computed energies indicate that amine-by-imine exchange is the most endothermic step of the hydrogenation reaction although, considering the unfavorable entropies associated with transition states **18TS** and **22TS** (see Supporting Information), any of the two other elementary steps in the cycle could become turnover-determining in the experimental system. In fact, the experimental rate law would agree with either a slow dissociative amine-by-imine exchange or a rate-determining bifunctional hydrogenation step. Moreover, the long induction periods observed under most experimental conditions likely reflect that the previous amine-assisted dihydrogen oxidative addition step becomes rate-determining at low amine concentrations. This concentration effect could be enhanced by competition of the imine for the hydrogen-bonding sites, which would account for the longer induction periods observed at higher initial imine concentrations.

With regard to the importance of hydrogen bonds in this mechanism, solvent properties should play a critical role in this catalysis, as is experimentally observed, although the overall effect of solvent seems difficult to rationalize. Thus, donor solvents are likely to compete with imine and amine for the reactive catalyst sites, but they can also strongly stabilize intermediates and polar transition states. Methanol, for example, forms hydrogen-bonded adducts with comparable stability and similar structure to those found with amine and imine (see Supporting Information). This analogy could be regarded as detrimental from the viewpoint of competition, but might also favor methanol-stabilized intermediates of the amine-by-imine exchange step.

Summary and Conclusion

The complex $[IrH_2(\eta^6\text{-}C_6H_6)(P\mathit{i}Pr_3)]BF_4$ (**1**) is an effective catalyst for the hydrogenation of *N*-benzylideneaniline under mild conditions. Less hindered aryl imines such as benzophenone imine deactivate the catalyst by substrate cyclometalation. The course of catalytic reactions is strongly dependent on concentrations, temperature, and solvents; methanol leads to the fastest hydrogenations. Most of the explored reaction conditions lead to pronounced activation periods, after which the rate law shows first-order dependences on dihydrogen pressure and catalyst and imine concentrations. Under hydrogenation conditions, precursor **1** transforms into the resting state $[IrH_2\{\eta^5\text{-}(C_6H_5)NHCH_2Ph\}(P\mathit{i}Pr_3)]BF_4$ (**3**), in which the hydrogenation product is coordinated to the metal through a phenyl ring. Complex **3** is activated by the amine product to initiate an ionic hydrogenation mechanism. Key steps in such a mechanism are: 1) Amine-assisted oxidative addition of dihydrogen, which formally corresponds to concerted addition to the iridium center but whose result is equivalent to heterolytic splitting of dihydrogen, 2) replacement of hydrogen-bonded amine by imine; and 3) simultaneous $H^{\delta+}/H^{\delta-}$ transfer to the imine from the NH moiety of the arene-coordinated amine ligand and the metal, respectively.

The present system illustrates how labile metal complexes can generate effective imine hydrogenation catalysts by exploiting the coordination and hydrogen-bonding capabilities of the components of these reactions. The deduced mechanism indicates that C=N bonds can indeed be hydrogenated by ionic outer-sphere bifunctional mechanisms similar to those found in C=O hydrogenation and transfer hydrogenation, whenever hydrides and protons can be effectively delivered to the metal and the proton-transferring functional group. In this latter respect, this work provides experimental and theoretical evidence for an alternative mechanism to accomplish such a proton and hydride delivery from dihydrogen, which is closely related to heterolytic splitting but formally different.

Experimental Section

Equipment: Infrared spectra were recorded on a Perkin-Elmer 883 (4000–200 cm^{-1}) or Bruker Equinox 55 (4000–400 cm^{-1}) spectrometer. C, H, N elemental analyses were carried out on a Perkin-Elmer 2400 CHNS/O analyzer. NMR spectra were recorded on Varian Gemini 2000 or Bruker Avance 400 or 300 MHz spectrometers. ^1H (400 or 300 MHz) and ^{13}C (100.6 or 75.5 MHz) NMR chemical shifts were measured relative to residual proton peaks of deuterated solvent but are reported in ppm relative to tetramethylsilane. ^{19}F (376.5 or 282.3 MHz) and ^{31}P (162.0 or 121.5 MHz) NMR chemical shifts were measured relative to $CFCl_3$ and H_3PO_4 (85%). Spectral assignments were achieved by ^1H-COSY and ^1H-NOESY, and ^{13}C-DEPT and ^1H,^{13}C-HMQC experiments. The temperature of the probe was calibrated by using the temperature dependence of the chemical shifts of methanol. Line-shape analysis of the spectra was performed with the g-NMR program. Errors in activation parameters obtained from the Eyring regression of the line-shape analysis rate constants assumed 1 K error in the temperature and 10% error in the constant, and were computed by published methods.[24] MS data were recorded on a VG Autospec double-focusing mass spectrometer operating in the positive mode; ions were produced with the Cs^+ gun at about 30 kV, and 3-nitrobenzyl alcohol (NBA) was used as the matrix. GC analyses were performed either on a Hewlett-Packard HP 5890 Series II gas chromatograph equipped with a flame ionization detector and a 25 m (0.32 mm inner diameter, 0.17 μm film thickness) HP-Ultra-1 column, or on an Agilent 6890 Series GC System equipped with an Agilent 5973 mass-selective detector and a 30 m (0.25 mm i.d., 0.25 μm f.t.) HP-5MS column.

Synthesis: All experiments were carried out under argon atmosphere by Schlenk techniques. Solvents were dried by known procedures and distilled under argon before use. Complexes $[IrH_2(\eta^6\text{-}C_6H_6)(P\textit{i}Pr_3)]BF_4$ (**1**),[12] $[IrH_2(NCMe)_3(P\textit{i}Pr_3)]BF_4$ (**2**),[11b] $[\{Ir(\mu\text{-}OMe)(cod)\}_2]$ (cod = 1,5-cyclooctadiene),[25] and phosphonium salt $[HP\textit{i}Pr_3]BF_4$[11b] were prepared as previously reported. Compounds **9**[11a] and **11**[12] were identified on the basis of previously reported characteristic data. *N*-Benzylideneaniline (Aldrich) was used as received in preparative reactions but was previously dried in solution with molecular sieves for several days when used in catalytic experiments (THF, 1,2-dicholoroethane) and reactions in NMR tubes. All other reagents were obtained from commercial sources and were used as received. All new compounds described below are air-sensitive in solution.

$[IrH_2\{\eta^5\text{-}(C_6H_5)NHCH_2Ph\}(P\textit{i}Pr_3)]BF_4$ (3): A suspension of $[\{Ir(\mu\text{-}OMe)(cod)\}_2]$ (127.6 mg, 0.19 mmol) in acetone (10 mL) was treated with $[HP\textit{i}Pr_3]BF_4$ (95.5 mg, 0.38 mmol) and $PhNHCH_2Ph$ (209.1 mg, 1.16 mmol). The resulting orange solution was stirred for 1 h under dihydrogen atmosphere, filtered through Celite, and concentrated to ca. 0.5 mL. Slow addition of diethyl ether produced a white solid, which was separated by decantation, washed with diethyl ether, and dried in vacuo (183.0 mg, 77%). ^1H NMR ([D$_6$]acetone, 243 K): $\delta = -17.04$ (dd, J(H,P) = 26.4, J(H,H) = 5.5 Hz, 1H; IrH), −16.87 (dd, J(H,P) = 26.4, J(H,H) = 5.5 Hz, 1H; IrH), 1.03 (dd, J(H,P) = 14.9, J(H,H) = 6.8 Hz, 9H; PCHCH_3), 1.05 (dd, J(H,P) = 14.8, J(H,H) = 6.9 Hz, 9H; PCHCH_3), 2.15 (m, 3H; PCHCH$_3$), 4.59 (dd, J(H,H) = 15.7, 6.4 Hz, 1H; CH$_2$), 4.68 (dd, J(H,H) = 15.7, 5.6 Hz, 1H; CH$_2$), 6.08 (d, J(H,H) = 6.5 Hz, 1H; η-CH), 6.30 (m, 2H; η-CH), 6.78 (t, J(H,H) = 7.0 Hz, 1H; η-CH), 6.80 (t, J(H,H) = 6.5 Hz, 1H; η-CH), 7.30–7.46 (m, 5H; CH), 7.53 (dd, J(H,H) = 6.4, 5.6 Hz, 1H; NH); $^{31}P\{^1H\}$ NMR ([D$_6$]acetone, 243 K): $\delta = 47.68$ (s); $^{13}C\{^1H\}$ NMR ([D$_6$]acetone, 243 K): $\delta = 19.16$, 19.32 (2×s; PCHCH_3), 27.38 (d, J(C,P) = 35.0 Hz; PCHCH$_3$), 45.66 (s; CH$_2$), 69.08 (d, J(C,P) = 2.8 Hz; η-CH), 72.96 (d, J(C,P) = 0.8 Hz; η-CH), 82.66, 101.12, 101.66 (all s; η-CH), 127.65, 128.88, 127.72 (all s; CH), 136.10, 144.33 (2×s; C); IR (KBr): $\tilde{\nu} = 3362$ (NH), 2208, 2180 cm^{-1} (IrH); MS (FAB+): m/z (%): 538 (100) [M^+]; elemental analysis calcd (%) for $C_{22}H_{36}NBF_4IrP$: C 42.31, H 5.81, N 2.24; found: C 41.86, H 6.11, N 2.14.

$[IrH\{PhN{=}CH(C_6H_4)\text{-}\kappa N,C\}(NCMe)_2(P\textit{i}Pr_3)]BF_4$ (4): A solution of **2** (361.0 mg, 0.64 mmol) in 1,2-dichloroethane (10 mL) was treated with PhN=CHPh (115.9 mg, 0.64 mmol) for 5 min at room temperature. Evolution of gas was observed immediately after addition. The resulting yellow solution was concentrated to ca. 0.5 mL, cooled to ca. 230 K, and treated with hexane (5 mL) to produce a yellow solid. The solid was separated by decantation, washed with hexane, and dried in vacuo (332.7 mg, 74%). ^1H NMR ($CDCl_3$, 293 K): $\delta = -20.39$ (dd, J(H,P) = 23.4, J(H,H) = 1.8 Hz, 1H; IrH), 0.94 (dd, J(H,P) = 13.8, J(H,H) = 6.9 Hz, 9H; PCHCH_3), 1.00 (dd, J(H,P) = 13.8, J(H,H) = 6.9 Hz, 9H; PCHCH_3), 1.96 (m, 3H; PCHCH$_3$), 2.37, 2.48 (2×s, 3H each; NCCH$_3$), 7.02–7.64 (m, 9H; CH), 8.50 (d, J(H,H) = 1.8 Hz, 1H; N=CH); $^{31}P\{^1H\}$ NMR ($CDCl_3$, 293 K): $\delta = 11.66$ (s); $^{13}C\{^1H\}$ NMR ($CDCl_3$, 293 K): $\delta = 3.32$ (s; NCCH_3), 3.35 (d, J(C,P) = 1.0 Hz; NCCH_3), 18.26 (d, J(C,P) = 1.5 Hz; PCHCH_3), 18.81 (d, J(C,P) = 1.4 Hz; PCHCH_3), 24.57 (d, J(C,P) = 33.5 Hz; PCHCH$_3$), 119.13 (d, J(C,P) = 16.9 Hz; NCCH_3), 120.96 (s; NCCH_3), 122.44, 122.50, 127.30, 129.58, 130.61, 132.45, 140.91 (all s; CH), 146.99, 150.62 (2×s; C), 148.70 (d, J(C,P) = 8.4 Hz; IrC), 176.30 (s; N=CH); ^{19}F NMR ($CDCl_3$, 293 K): $\delta = -154.8$ (s); IR (KBr): $\tilde{\nu} = 2196$ cm^{-1} (IrH); MS (FAB+): m/z (%): 615 (4) [M^+], 574 (20) [M^+−NCMe], 533 (100) [M^+−2NCMe]; elemental analysis calcd (%) for $C_{26}H_{38}N_3BF_4IrP$: C 44.45, H 5.45, N 5.98; found: C 44.20, H, 5.49, N 5.95.

$[IrH\{PhN{=}CH(C_6H_4)\text{-}\kappa N,C\}(NCMe)(NH_2Ph)(P\textit{i}Pr_3)]BF_4$ (5): A solution of **4** (332.7 mg, 0.47 mmol) in 1,2-dichloroethane (10 mL) was treated with aniline (43.1 μL, 0.47 mmol) and stirred for 5 min at room temperature. The resulting brown solution was concentrated to ca. 0.5 mL and layered with hexane to afford yellow crystals (239.4 mg, 67%). ^1H NMR ($CDCl_3$, 293 K): $\delta = -20.53$ (dd, J(H,P) = 23.1, J(H,H) = 1.9 Hz, 1H; IrH), 0.92 (dd, J(H,P) = 14.1, J(H,H) = 7.2 Hz, 9H; PCHCH_3), 0.97 (dd, J(H,P) = 14.1, J(H,H) = 7.2 Hz, 9H; PCHCH_3), 2.01 (m, 3H; PCHCH$_3$), 2.56 (s, 3H; NCCH$_3$), 4.98 (dd, J(H,H) = 11.1, J(H,P) = 4.3 Hz, 1H; NH), 5.98 (dd, J(H,H) = 11.1, J(H,P) = 4.3 Hz, 1H; NH), 6.39 (m, 2H; CH), 6.91, 7.37 (2×m, 5H each; CH), 7.54 (m, 2H; CH), 8.38 (d, J(H,H) = 1.9 Hz, 1H; N=CH); $^{31}P\{^1H\}$ NMR ($CDCl_3$, 293 K): $\delta = 14.60$ (s); $^{13}C\{^1H\}$ NMR ($CDCl_3$, 293 K): $\delta = 3.65$ (s; NCCH_3), 18.39 (d, J(C,P) = 1.5 Hz; PCHCH_3), 18.86 (d, J(C,P) = 2.0 Hz; PCHCH_3), 25.01 (d, J(C,P) = 32.4 Hz; PCHCH$_3$), 120.60, 120.22 (2×s; CH), 122.27 (s; NCCH_3), 122.77, 124.00, 127.47, 128.08, 129.33, 130.99, 132.59, 141.17 (all s; CH), 141.64 (d, J(C,P) = 2.0 Hz; C), 146.95, 150.68 (2×s; C), 154.46 (d, J(C,P) = 7.9 Hz; IrC), 176.20 (s; N=CH); ^{19}F NMR ($CDCl_3$, 293 K): $\delta = -154.1$ (s); IR (KBr): $\tilde{\nu} = 3300$, 3255 (NH), 2194 cm^{-1} (IrH); MS (FAB+): m/z (%): 626 (30) [M^+−NCMe], 533 (100) [M^+−NCMe−NH$_2$Ph]; elemental analysis calcd (%) for $C_{30}H_{42}N_3BF_4IrP$: C 47.25, H 5.60, N 5.56; found: C 47.70, H 5.89, N 5.45.

$[Ir\{HN{=}CPh(C_6H_4)\text{-}\kappa N,C\}_2(NH_2CHPh_2)(P\textit{i}Pr_3)]BF_4$ (6): A solution of **2** (36.1 mg, 0.06 mmol) in $CDCl_3$ (0.5 mL) was treated with $HN{=}CPh_2$ (115.9 mg, 0.64 mmol) and H_2 (1 bar) at 328 K in a Wilmad NMR tube equipped with a J-Young valve. After 1 h of reaction, the NMR spectra of the resulting solution revealed quantitative formation of **6**. The solution was transferred to a Schlenk tube and taken to dryness, and the residue was stirred with diethyl ether to give a yellow solid. The solid was separated by decantation, washed with diethyl ether, and dried in vacuo (46.0 mg, 78%). ^1H NMR ($CDCl_3$, 293 K): $\delta = 0.84$ (dd, J(H,P) = 13.2 Hz; J(H,H) = 7.2 Hz, 18H; PCHCH_3), 1.98 (m, 3H; PCHCH$_3$), 3.53 (dd, J(H,H) = 4.6, J(H,P) = 3.0 Hz, 2H; NH$_2$), 4.52 (td, J(H,H) = 4.6, J(H,P) = 3.6 Hz, 1H; NH$_2$CH), 6.50, 6.90 (2×m, 4H each; CH), 6.99 (t, J(H,H) = 7.4 Hz, 4H; CH), 7.14 (dd, J(H,H) = 7.6, 1.2 Hz, 4H; CH), 7.32 (m, 4H; CH), 7.41–7.47 (m, 6H; CH), 8.64 (d, J(H,H) = 7.5 Hz, 2H; CH), 10.62 (s, 2H; NH); $^{31}P\{^1H\}$ NMR ($CDCl_3$, 293 K): $\delta = -7.58$ (s); $^{13}C\{^1H\}$ NMR ($CDCl_3$, 293 K): $\delta = 18.85$ (s; PCHCH_3), 25.09 (d, J(C,P) = 30.4 Hz; PCHCH$_3$), 63.23 (s; NH$_2$CH), 122.69, 126.17, 126.92, 128.29, 128.52, 128.74, 130.56, 130.99, 132.32 (all s; CH), 136.26 (s; C), 137.67 (s; CH), 141.86, 148.50 (2×s; C), 154.23 (d, J(C,P) = 7.8 Hz; IrC), 189.78 (s; N=C); MS (FAB+): m/z (%): 896 (9) [M^+], 713 (89) [M^+−NH$_2$CHPh$_2$]; elemental analysis calcd (%) for $C_{48}H_{54}N_3BF_4IrP$: C 58.65, H 5.54, N 4.27; found: C 58.53, H 5.74, N 4.09;

$[IrH\{PhN{=}CH(C_6H_4)\text{-}\kappa N,C\}([D_6]acetone)_2(P\textit{i}Pr_3)]BF_4$ (7): A solution of **1** (62.8 mg, 0.12 mmol) in [D$_6$]acetone (0.5 mL) was treated with PhN=CHPh (21.9 mg, 0.12 mmol) for 1 h at 273 K in a NMR tube. The NMR spectrum of the resulting solution revealed the formation of complexes **7** and **3** in a 62:38 molar ratio, together with benzene and traces of *N*-benzylaniline and **9**. Selected NMR data for **7**: ^1H NMR ([D$_6$]acetone,

233 K): $\delta = -20.08$ (dd, J(H,P) = 25.2, J(H,H) = 1.6 Hz, 1H; IrH), 0.93 (dd, J(H,P) = 14.4, J(H,H) = 6.9 Hz, 9H; PCHCH_3), 2.00 (m, 3H; PCHCH$_3$), 6.99, 7.96 (2×m, 2H each; CH), 8.90 (d, J(H,H) = 1.6 Hz, 1H; N=CH); ^{31}P{^{1}H} NMR ([D$_6$]acetone, 233 K): $\delta = 15.06$ (s); ^{13}C{^{1}H} NMR ([D$_6$]acetone, 233 K): $\delta = 18.80$, 19.51 (2×s; PCHCH$_3$), 25.20 (d, J(C,P) = 35.1 Hz; PCHCH$_3$), 123.54, 124.29, 130.07, 130.28, 132.32, 133.06 (all s; CH), 142.14 (d, J(C,P) = 7.5 Hz; IrC), 143.28 (s; CH), 148.37, 152.00 (2× s; C), 177.90 (s; N=CH), 226.57 (s; CO).

[IrH{PhN=CH(C$_6$H$_4$)-$\kappa N,C$}([D$_4$]methanol)$_2$(PiPr$_3$)]BF$_4$ (8): A solution of **1** (62.8 mg, 0.12 mmol) in methanol (5 mL) was treated with PhN=CHPh (21.9 mg, 0.12 mmol) at room temperature under reduced pressure until the solvent had totally evaporated. The resulting residue was repeatedly washed with diethyl ether to obtain a red oil. The NMR analysis of the oil revealed the presence of complex **8** and its isotopomer deuterated at the hydride position, together with minor amounts (ca. 3% of each) of *N*-benzylaniline, **3**, and **10** (see below). Selected NMR data for **8**: ^{1}H NMR ([D$_4$]methanol, 293 K): $\delta = -20.39$ (dd, J(H,P) = 25.6, J(H,H) = 0.9 Hz, 1H; IrH), 1.15 (dd, J(H,P) = 13.9, J(H,H) = 7.3 Hz, 9H; PCHCH_3), 1.22 (dd, J(H,P) = 13.9, J(H,H) = 7.3 Hz, 9H; PCHCH_3), 2.22 (m, 3H; PCHCH$_3$), 7.12 (t, J(H,H) = 5.1 Hz, 2H; CH), 7.50 (t, J(H,H) = 6.6 Hz, 1H; CH), 7.62 (m, 4H; CH), 7.73 (m, 2H; CH), 8.93 (d, J(H,H) = 0.9 Hz, 1H; N=CH); ^{31}P{^{1}H} NMR ([D$_4$]methanol, 293 K): $\delta =$ 14.31 (s); ^{13}C{^{1}H} NMR ([D$_4$]methanol, 293 K): $\delta = 19.11$ (d, J(C,P) = 1.5 Hz; PCHCH$_3$), 19.67 (d, J(C,P) = 2.2 Hz; PCHCH$_3$), 25.80 (d, J(C,P) = 35.1 Hz; PCHCH$_3$), 123.51, 124.02, 128.53, 130.69, 132.40, 133.39 (all s; CH), 141.95 (d, J(C,P) = 7.3 Hz, IrC), 142.95 (s; CH), 148.70, 152.91 (2×s; C), 178.89 (s; N=CH); ^{19}F NMR ([D$_4$]methanol, 293 K): $\delta =$ −154.3 (s); MS (FAB+): m/z (%): 598 (20) [M^+], 534 (90) [M^+ −2 CH$_3$OH].

Reaction of 7 or 8 with H$_2$: A [D$_6$]acetone solution (0.9 mL) of **7** was generated in an NMR tube by reaction of **1** (31.4 mg, 0.06 mmol) with excess PhN=CHPh (115.9 mg, 0.64 mmol) at 293 K. Benzene and *N*-benzylaniline were also formed in the reaction (NMR). H$_2$ (1 bar) was bubbled through the solution for 15 min at room temperature. Complex **3** and *N*-benzylaniline were the only products detectable by NMR spectroscopy in the resulting solution. The same results were obtained with a [D$_4$]methanol solution of **8** generated in a similar way.

[IrH$_2$(CD$_3$OD)$_3$(PiPr$_3$)]BF$_4$ (10): The NMR spectra of [D$_4$]methanol solutions of **1** showed the quantitative evolution of the precursor complex into benzene and complex **10**. Selected data for **10**: ^{1}H NMR ([D$_4$]methanol, 293 K): $\delta = -32.47$ (d, J(H,P) = 24.9 Hz, 2H; IrH), 1.32 (dd, J(H,P) = 13.8, J(H,H) = 7.5 Hz, 18H; PCHCH_3), 2.30 (m, 3H; PCHCH$_3$); ^{31}P{^{1}H} NMR ([D$_4$]methanol, 293 K): $\delta = 32.11$ (s); ^{13}C{^{1}H} NMR ([D$_4$]methanol, 293 K): $\delta = 20.05$ (d, J(C,P) = 0.9 Hz; PCHCH$_3$), 26.50 (d, J(C,P) = 35.9 Hz; PCHCH$_3$); ^{19}F NMR ([D$_4$]methanol, 293 K): $\delta = -151.3$ (s).

Reaction of 8 with H$_2$ and NaBPh$_4$ in [D$_4$]methanol: A solution of **8** in [D$_4$]methanol (0.5 mL), generated in a NMR tube from **1** (20.20 mg, 0.04 mmol) and PhN=CHPh (7.05 mg, 0.04 mmol) as described above, was treated with NaBPh$_4$ (13.31 mg, 0.04 mmol). The resulting solution was analyzed by NMR spectroscopy to check the integrity of complex **8**. Then, the solution was allowed to react with dihydrogen at atmospheric pressure, which caused the immediate precipitation of a white solid. The solid and solution were separated by centrifugation of the NMR tube and analyzed. The [D$_4$]methanol solution was found to contain a PhN=CHPh/PhNHCH$_2$Ph mixture in a molar ratio of 90:10. The solid was dissolved in CDCl$_3$ and identified as **11** by comparison of its NMR data with those previously published.[12] Similar experiments were carried out starting from **7** in [D$_6$]acetone, or **4** in CD$_2$Cl$_2$, to obtain equivalent results. In these cases, **11** was soluble in the reaction media.

[Ir$_2$(μ-Cl)(μ-H)ClH{PhN=CH(C$_6$H$_4$)-$\kappa N,C$}$_2$(PiPr$_3$)$_2$] (12): A solution of **1** (150.0 mg, 0.29 mmol) in CHCl$_3$ (5 mL) was treated with PhN=CHPh (55.6 mg, 0.29 mmol) for 2 d at 323 K. The resulting dark red solution was evaporated to dryness and the residue was extracted with diethyl ether (10 mL). The solvent was removed in vacuo and the resulting oil was treated with hexane at 213 K to give an orange solid, which was separated by decantation, washed with hexane, and dried in vacuo (198.1 mg, 60%). ^{1}H NMR (CDCl$_3$, 293 K): $\delta = -19.22$ (d, J(H,P) = 15.2 Hz, 1H; IrH), −16.93 (dd, J(H,P) = 46.0, 12.1 Hz, 1H; IrHIr), 0.83 (dd, J(H,P) = 15.1, J(H,H) = 7.6 Hz, 9H; PCHCH_3), 0.86 (dd, J(H,P) = 14.4, J(H,H) = 7.3 Hz, 9H; PCHCH_3), 1.00 (dd, J(H,P) = 13.9, J(H,H) = 6.9 Hz, 9H; PCHCH_3), 1.07 (dd, J(H,P) = 14.4, J(H,H) = 6.9 Hz, 9H; PCHCH_3), 1.40, 2.20 (2×m, 3H each; PCHCH$_3$), 6.85 (d, J(H,H) = 6.1 Hz, 1H; CH), 7.00 (d, J(H,H) = 8.1 Hz, 1H; CH), 7.08 (m, 2H; CH), 7.21, 7.32 (2×m, 3H each; CH), 7.38 (m, 2H; CH), 7.54 (d, J(H,H) = 7.6 Hz, 2H; CH), 7.69 (d, J(H,H) = 7.6 Hz, 2H; CH), 7.95 (d, J(H,H) = 6.6 Hz, 2H; CH), 8.77, 8.99 (2×s, 1H each; N=CH); ^{31}P{^{1}H} NMR (CDCl$_3$, 293 K): $\delta = 20.20$, 22.23 (2×s); ^{13}C{^{1}H} NMR (CDCl$_3$, 293 K): $\delta = 18.38$ (d, J(C,P) = 1.4 Hz; PCHCH$_3$), 18.53 (s; PCHCH$_3$), 18.63 (d, J(C,P) = 2.1 Hz; PCHCH$_3$), 19.44 (d, J(C,P) = 1.6 Hz; PCHCH$_3$), 25.27 (d, J(C,P) = 30.6 Hz; PCHCH$_3$), 25.44 (d, J(C,P) = 31.0 Hz; PCHCH$_3$), 122.65, 122.99, 123.84, 125.17 (all s; CH), 126.23 (d, J(C,P) = 6.3 Hz; IrC), 128.31, 128.87, 128.90, 129.80, 129.84, 130.43, 131.27, 131.49, 131.77, 132.62, 138.86, 139.30 (all s; CH), 144.74 (s; C), 145.31 (d, J(C,P) = 7.5 Hz; IrC), 146.51, 148.03, 150.57 (all s; C), 175.13, 176.63 (2×s; N=CH); IR (KBr): $\tilde{\nu} = 2031$ (IrH), 1956 cm^{-1} (Ir-H-Ir); MS (FAB+): m/z (%): 1137 (29) [M^+−H], 1103 (62) [M^+−Cl]; elemental analysis calcd (%) for C$_{44}$H$_{64}$N$_2$Cl$_2$Ir$_2$P$_2$: C 46.43, H 5.67, N 2.46; found: C 46.85, H 5.70, N 2.36.

[Ir$_2$(μ-Cl)(μ-H)Cl$_2${PhN=CH(C$_6$H$_4$)-$\kappa N,C$}$_2$(PiPr$_3$)$_2$] (13): A solution of **12** (100.0 mg, 0.09 mmol) in CHCl$_3$ (5 mL) was stirred for 24 h at 323 K. The solvent was removed in vacuo and the resulting residue was treated with hexane at 213 K to give a dark orange solid, which was separated by decantation, washed with hexane, and dried in vacuo (82.4 mg, 80%). ^{1}H NMR (CDCl$_3$, 293 K): $\delta = -19.97$ (dd, J(H,P) = 50.4 Hz, 10.8, 1H; IrHIr), 0.69 (dd, J(H,P) = 14.4, J(H,H) = 7.2 Hz, 9H; PCHCH_3), 0.78 (dd, J(H,P) = 14.1, J(H,H) = 7.1 Hz, 9H; PCHCH_3), 0.99 (dd, J(H,P) = 14.6, J(H,H) = 7.1 Hz, 9H; PCHCH_3), 1.11 (dd, J(H,P) = 14.1, J(H,H) = 7.1 Hz, 9H; PCHCH_3), 2.00, 2.33 (2×m, 3H each; PCHCH$_3$), 6.96 (t, J(H,H) = 7.2 Hz, 1H; CH), 7.10 (d, J(H,H) = 7.5 Hz, 1H; CH), 7.19 (m, 3H; CH), 7.24 (d, J(H,H) = 6.6 Hz, 1H; CH), 7.38 (t, J(H,H) = 7.3 Hz, 2H; CH), 7.44 (d, J(H,H) = 7.1 Hz, 1H; CH), 7.51 (m, 3H; CH), 7.64 (d, J(H,H) = 7.5 Hz, 2H; CH), 7.73 (d, J(H,H) = 6.6 Hz, 1H; CH), 7.80 (d, J(H,H) = 7.1 Hz, 2H; CH), 7.98 (d, J(H,H) = 7.1 Hz, 1H; CH), 8.57, 8.67 (2×s, 1H each; N=CH); ^{31}P{^{1}H} NMR (CDCl$_3$, 293 K): $\delta = 8.17$, 12.21 (2×s); ^{13}C{^{1}H} NMR (CDCl$_3$, 293 K): $\delta = 18.55$ (d, J(C,P) = 2.0 Hz; PCHCH$_3$), 19.09 (d, J(C,P) = 3.1 Hz; PCHCH$_3$), 19.17 (d, J(C,P) = 2.7 Hz; PCHCH$_3$), 19.41 (d, J(C,P) = 2.0 Hz; PCHCH$_3$), 25.68 (d, J(C,P) = 31.0 Hz; PCHCH$_3$), 25.78 (d, J(C,P) = 29.5 Hz; PCHCH$_3$), 123.91, 124.31, 124.62, 125.44, 128.70, 128.80, 128.91, 129.28, 131.58, 132.20, 133.19, 134.83, 140.10 (all s; CH), 141.37 (d, J(C,P) = 6.5 Hz; IrC), 141.52 (d, J(C,P) = 6.9 Hz; IrC), 146.84, 147.67, 149.75, 150.44 (all s; C), 179.69, 182.58 (2×s; N=CH); IR (KBr): $\tilde{\nu} = 2031$ cm^{-1} (Ir-H-Ir); MS (FAB+): m/z (%): 1172 (20) [M^+], 1137 (100) [M^+−Cl]; elemental analysis calcd (%) for C$_{44}$H$_{63}$N$_2$Cl$_3$Ir$_2$P$_2$: C 45.07, H 5.41, N 2.39; found: C 44.67, H 5.76, N 2.37.

[IrH$_2${η^5-(C$_6$H$_5$)NCH$_2$Ph}(PiPr$_3$)] (14): A suspension of **3** (46.9 mg, 0.07 mmol) in [D$_8$]THF (0.5 mL) in an NMR tube was cooled to ca. 200 K and treated with NaH (1.8 mg, 0.07 mmol). Fast evolution of gas was observed immediately after addition. The remaining solid was separated by centrifugation in the NMR tube, and the resulting yellow solution was analyzed by NMR spectroscopy. Complex **14** was the sole component of the solution. ^{1}H NMR ([D$_8$]THF, 293 K): $\delta = -18.77$ (dd, J(H,P) = 27.6, J(H,H) = 5.7 Hz, 1H; IrH), −18.31 (dd, J(H,P) = 27.6, J(H,H) = 5.7 Hz, 1H; IrH), 1.14 (dd, J(H,P) = 14.0, J(H,H) = 7.1 Hz, 18H; PCHCH_3), 2.12 (m, 3H; PCHCH$_3$), 4.48 (AB spin system: δ(A) = 4.46, δ(B) = 4.51, J(A,B) = 16.2 Hz, 2H; CH$_2$), 5.02 (d, J(H,H) = 6.7 Hz, 1H; η-CH), 5.07 (d, J(H,H) = 7.2 Hz, 1H; η-CH), 5.52 (t, J(H,H) = 6.1 Hz, 1H; η-CH), 5.64 (t, J(H,H) = 6.1 Hz, 1H; η-CH), 5.75 (t, J(H,H) = 6.2 Hz, 1H; η-CH), 7.20 (t, J(H,H) = 7.5 Hz, 2H; CH), 7.29 (t, J(H,H) = 7.4 Hz, 1H; CH), 7.35 (d, J(H,H) = 7.5 Hz, 2H; CH); ^{31}P{^{1}H} NMR ([D$_8$]THF, 293 K): $\delta = 43.03$ (s); ^{13}C{^{1}H} NMR ([D$_8$]THF, 283 K): $\delta = 21.28$, 21.49 (2×s; PCHCH$_3$), 29.15 (d, J(C,P) = 32.2 Hz; PCHCH$_3$), 52.10 (s; CH$_2$), 65.73, 76.49, 91.69, 99.62 (all s; η-CH), 126.97, 129.06, 129.11 (all s; CH), 135.43, 141.99 (2×s; C).

X-ray structure analysis of 3, 5, and 6: Crystals suitable for these experiments were obtained by slow diffusion of diethyl ether and hexane at

253 K into CH_2Cl_2 solutions of **3** and **5**, respectively, and by diffusion of benzene/diethyl ether into a $CDCl_3$ solution of **6**. X-ray data were collected on a Bruker SMART APEX CCD diffractometer with graphite-monochromated $Mo_{K\alpha}$ radiation ($\lambda = 0.71073$ Å) using ω scans (0.3°). Data were collected over the complete sphere by a combination of four sets, and corrected for absorption by a multiscan method applied with the SADABS program.[26] The structures were solved by the Patterson method. Refinement by full-matrix least-squares methods on F^2 using SHELXL97[27] was similar for all complexes and included isotropic and subsequently anisotropic displacement parameters for all nondisordered non-hydrogen atoms. Particular details concerning the presence of solvent, static disorder, and hydrogen refinement are listed below.

Crystal data for 3: $C_{22}H_{36}BF_4IrNP\cdot 0.25\,H_2O$, $M = 629.00$; colorless needle, $0.28 \times 0.04 \times 0.04$ mm; triclinic, $P\bar{1}$; $a = 7.7841(7)$, $b = 11.5325(11)$, $c = 14.1366(13)$ Å, $\alpha = 75.6620(10)$, $\beta = 77.545(2)$, $\gamma = 84.674(2)°$; $Z = 2$; $V = 1199.54(19)$ Å^3; $\rho_{calcd} = 1.741$ g cm^{-3}; $\mu = 5.673$ mm^{-1}, min/max transmission factors 0.474/0.612; $2\theta_{max} = 56.9°$; $T = 100.0(2)$ K; 14275 reflections collected, 5506 unique (R(int) = 0.034); number of data/restraints/parameters 5506/1/301; final GoF 1.067, $R1 = 0.0424$ [4754 reflections with $I > 2\sigma(I)$], $wR2 = 0.1050$ (all data); largest difference peak 4.358 e Å^{-3}. Hydrogen atoms were included in calculated positions and refined riding on carbon atoms with the thermal parameter related to bonded atoms or with very weak positional restraints. The highest electronic residual was observed as an unique peak sitting in the middle of a structural hole formed by two terminal phenyl rings and several isopropyl groups belonging to four different molecules. This residue shows short distances (about 2.6 Å) with both aliphatic and aromatic C–H bonds, and was interpreted as 0.25 molecules of water of crystallization.

Crystal data for 5: $C_{30}H_{42}BF_4IrN_3P\cdot CH_2Cl_2$, $M = 839.57$; yellow irregular block, $0.28 \times 0.12 \times 0.12$ mm; triclinic, $P\bar{1}$; $a = 10.2813(7)$, $b = 13.5231(9)$, $c = 13.9998(9)$ Å, $\alpha = 103.8940(10)$, $\beta = 102.4430(10)$, $\gamma = 108.4630(10)°$; $Z = 2$; $V = 1700.1(2)$ Å^3; $\rho_{calcd} = 1.640$ g cm^{-3}; $\mu = 4.179$ mm^{-1}, min/max transmission factors 0.396/0.593; $2\theta_{max} = 57.2°$; $T = 100.0(2)$ K; 20336 reflections collected, 7901 unique (R(int) = 0.0281); number of data/restraints/parameters 7901/5/411; final GoF 0.972, $R1 = 0.0267$ [7021 reflections with $I > 2\sigma(I)$], $wR2 = 0.0596$ (all data); largest difference peak 1.805 e Å^{-3}. Hydrogen atoms were included in calculated positions and refined riding on carbon atoms or in observed positions and refined freely with the thermal parameter related to bonded atoms. The highest electronic residual was observed in close proximity of the disordered solvent molecule.

Crystal data for 6: $C_{48}H_{54}BF_4IrN_3P\cdot 0.6\,C_4H_{10}O\cdot 0.3\,CHCl_3\cdot 0.25\,C_6H_6$, $M = 1082.73$; yellow plate, $0.14 \times 0.12 \times 0.04$ mm; triclinic, $P\bar{1}$; $a = 10.9839(11)$, $b = 11.6980(12)$, $c = 19.996(2)$ Å, $\alpha = 95.622(2)$, $\beta = 90.785(2)$, $\gamma = 105.855(2)°$; $Z = 2$; $V = 2457.5(4)$ Å^3; $\rho_{calcd} = 1.463$ g cm^{-3}; $\mu = 2.853$ mm^{-1}, min./max. transmission factors 0.648 and 0.803; $2\theta_{max} = 57.0°$; $T = 100.0(2)$ K; 24254 reflections collected, 11170 unique (R(int) = 0.0812); number of data/restraints/parameters 11170/28/577; final GoF 0.755, $R1 = 0.0534$ [5970 reflections with $I > 2\sigma(I)$], $wR2 = 0.1209$ (all data); largest difference peak 1.499 e Å^{-3}. Two solvent molecules (diethyl ether and chloroform) were observed disordered in the same site of the crystal. Both molecules were refined with restraints on their geometry. The occupancy factors were estimated from thermal parameters and fixed to 0.6 for the diethyl ether and to 0.3 for the chloroform moiety. One benzene molecule was also observed around a center of symmetry. Its occupancy factor was estimated from the thermal parameters and fixed to 0.25. Hydrogen atoms were included in calculated positions and refined riding on carbon atoms or in observed positions and refined freely. The largest electronic residuals were observed in the proximity of the solvent molecules.

CCDC-285459, -285460, and -285461 contain the supplementary crystallographic data for this paper. These data can be obtained free of charge from the Cambridge Crystallographic Data Centre via www.ccdc.cam.ac.uk/data_request/cif.

Catalytic hydrogenation: Dihydrogen-uptake experiments were performed in an apparatus consisting of a 7.99 mL stainless-steel gas reservoir triply connected to a high-pressure dihydrogen source, a pressure transmitter, and a electronic pressure meter/controller (EL-Press, Bronkhorst HI-TEC). The outlet of the pressure controller was connected to a 100 mL reaction flask, also connected to a Schlenk manifold to allow for manipulation of the reaction under argon and degassing. In a typical reaction, a solution of the catalyst precursor and the substrate at the desired concentrations was transferred to the reaction flask and allowed to reach the reaction temperature in a water bath. The reaction mixture was degassed in vacuo over a few seconds and exposed to dihydrogen at the desired total pressure. The pressure was programmed on the computer connected to the pressure controller, which maintains a constant pressure in the reaction flask during hydrogenation. The reaction flask was shaken vigorously during reaction. Consumption of dihydrogen was registered as a pressure decrease in the closed reservoir by means of the pressure transmitter at the desired intervals (typically 15 s). The pressure decrease was converted into moles of dihydrogen consumed by using the precalibrated volume of the reservoir and considering ideal gas behavior. The data were fitted to exponentials, where applicable, to obtain extrapolated initial rate data and pseudo-first-order rate constants. The vapor pressure of the solvent at the reaction temperature was considered in calculating dihydrogen partial pressures.[28] The reaction progress and selectivity were periodically checked by GC on samples obtained through the septum cap of the reaction flask. The imine/amine ratio was calculated from the GC peaks by using the regression plot previously obtained from known solutions of both commercial substrates in the same range of concentrations.

Preparation of NMR samples of catalytic reactions: The hydrogenation procedure described above was applied to solutions in the desired deuterated solvent (typically 2 mL of solvent, at least 15 mg of the catalyst precursor, an initial substrate to catalyst ratio of 20, and dihydrogen total pressure of 1.1 bar). The reactions were monitored by means of dihydrogen consumption until the desired conversion (typically 50%) and then transferred with a cannula, under dihydrogen, to NMR tubes. The NMR tubes were frozen, and the $^{31}P\{^1H\}$ NMR spectra measured (typically at 273 K, at which temperature the reaction is slow enough to ensure that an excess of all reaction components is maintained during the measurement).

Calculations: Theoretical calculations were carried out with the Gaussian program suite.[29] The presented structures were fully optimized by second-order Møller–Plesset perturbation theory (MP2) with two different basis sets: basis-I and basis-II. Basis-I is a valence double-ζ quality basis set, and basis-II includes polarization functions. All the presented structures were fully optimized at the MP2/basis-I level of theory. Harmonic vibrational frequency calculations at this level of theory were used to characterize these structures as either minima (zero imaginary harmonic frequencies) or transition states (a single imaginary harmonic frequency), and these energy second derivatives were used to estimate the Gibbs free energy. Then, these structures were reoptimized at the MP2/basis-II level of theory, and natural population analysis (NPA) was used to estimate the atomic charges.

Basis-I includes the valence double-ζ Dunning–Huzinaga[30] basis for B, C, N, O, F, and H atoms, and the Hay–Wadt effective core potential and valence basis set for Ir[31] and P[32] atoms. Basis-II includes one set of polarization functions for the first-row and selected H atoms, and the extended Hay–Wadt effective core potential for Ir and P atoms,[33] supplemented with polarization d functions for the P atom[34] and a diffuse d function[35] and a polarization f function[36] for the Ir atom.

Acknowledgements

This research was supported by Plan Nacional de Investigación MEC/FEDER (Project BQU2003-05412).

[1] Reviews on imine hydrogenation: a) B. R. James, *Catal. Today* **1997**, *37*, 209–221; b) H.-U. Blaser, F. Spindler in *Comprehensive Asymmetric Catalysis, Vol. 1* (Eds.: E. N. Jacobsen, A. Pfaltz, H. Yamamoto), Springer, New York, **1999**, pp. 247–265; c) S. Kobayashi, H. Ish-

itani, *Chem. Rev.* **1999**, *99*, 1069–1094; d) W. Tang, X. Zhang, *Chem. Rev.* **2003**, *103*, 3029–3069.

[2] For leading references and important patents, see a) H.-U. Blaser, E. Schmidt, *Asymmetric Catalysis on Industrial Scale: Challenges, Approaches and Solutions*, Wiley-VCH, Weinheim, **2004**; b) R. Dorta, D. Broggini, R. Stoop, H. Rüegger, F. Spindler, A. Togni, *Chem. Eur. J.* **2004**, *10*, 267–278; c) E. Guiu, B. Muñoz, S. Castillón, C. Claver, *Adv. Synth. Catal.* **2003**, *345*, 169–171; d) B. Pugin, H. Landert, F. Spindler, H.-U. Blaser, *Adv. Synth. Catal.* **2002**, *344*, 974–979.

[3] a) A. Baranyai, F. Ungváry, L. Markó, *J. Mol. Catal.* **1985**, *32*, 343–348; b) C. J. Longley, T. J. Goodwin, G. Wilkinson, *Polyhedron* **1986**, *5*, 1625–1628; c) H.-A. Brune, J. Unsin, R. Hemmer, M. Reichhardt, *J. Organomet. Chem.* **1989**, *369*, 335–342; d) A. G. Becalski, W. R. Cullen, M. D. Fryzuk, B. R. James, G.-J. Kang, S. J. Rettig, *Inorg. Chem.* **1991**, *30*, 5002–5008; e) E. Baralt, S. J. Smith, J. Hurwitz, I. T. Horváth, R. H. Fish, *J. Am. Chem. Soc.* **1992**, *114*, 5187–5196; f) C. A. Willoughby, S. L. Buchwald, *J. Am. Chem. Soc.* **1994**, *116*, 8952–8965.

[4] For examples of unusual imine insertion into M–H and M–C bonds, see a) F. Liang, H. W. Schmalle, H. Berke, *Inorg. Chem.* **2004**, *43*, 993–999; b) D. Lafrance, J. L. Davids, R. Dhawan, B. A. Arndtsen, *Organometallics* **2001**, *20*, 1128–1136; c) R. D. Dghaym, K. J. Yaccato, B. A. Arndtsen, *Organometallics* **1998**, *17*, 4–6; d) S. Kacker, J. S. Kim, A. Sen, *Angew. Chem.* **1998**, *110*, 1335–1337; *Angew. Chem. Int. Ed.* **1998**, *37*, 1251–1253; e) Y. Obora, T. Ohta, C. L. Stern, T. J. Marks, *J. Am. Chem. Soc.* **1997**, *119*, 3745–3755; f) M. D. Fryzuk, W. E. Piers, *Organometallics* **1990**, *9*, 986–998.

[5] R. M. Bullock, *Chem. Eur. J.* **2004**, *10*, 2366–2374.

[6] a) Y. N. C. Chan, J. A. Osborn, *J. Am. Chem. Soc.* **1990**, *112*, 9400–9401; b) C. A. Willoughby, S. L. Buchwald, *J. Am. Chem. Soc.* **1994**, *116*, 11703–11714; c) V. Herrera, B. Muñoz, V. Landaeta, N. Canudas, *Mol. Catal. A* **2001**, *174*, 141–149.

[7] a) C. P. Casey, J. B. Johnson, *J. Am. Chem. Soc.* **2005**, *127*, 1883–1894; b) H. Guan, M. Iimura, M. P. Magee, J. Norton, G. Zhu, *J. Am. Chem. Soc.* **2005**, *127*, 7805–7814; c) X.-Y Liu, K. Venkatesan, H. W. Schmalle, H. Berke, *Organometallics* **2004**, *23*, 3153–3163; d) C. P. Casey, S. W. Singer, D. R. Powell, R. K. Hayashi, M. Kavana, *J. Am. Chem. Soc.* **2001**, *123*, 1090–1100. See also: e) D. Xiao, X. Zhang, *Angew. Chem.* **2001**, *113*, 3533–3536; *Angew. Chem. Int. Ed.* **2001**, *40*, 3425–3428.

[8] a) K. Abdur-Rashid, S. E. Clapham, A. Hadzovic, J. N. Harvey, A. J. Lough, R. H. Morris, *J. Am. Chem. Soc.* **2002**, *124*, 15104–15118; b) C. A. Sandoval, T. Ohkuma, K. Muñiz, R. Noyori, *J. Am. Chem. Soc.* **2003**, *125*, 13490–13503; see also: c) R. Noyori, M. Yamakawa, S. Hashiguchi, *J. Org. Chem.* **2001**, *66*, 7931–7944; d) J. S. M. Samec, J.-E. Bäckwall, *Chem. Eur. J.* **2002**, *8*, 2955–2961.

[9] S. E. Clapham, A. Hadzovic, R. H. Morris, *Coord. Chem. Rev.* **2004**, *248*, 2201–2237.

[10] M. Martín, E. Sola, S. Tejero, J. A. López, L. A. Oro, *Chem. Eur. J.* **2006**, *12*, 4057–4068.

[11] a) F. Torres, E. Sola, M. Martín, J. A. López, F. J. Lahoz, L. A. Oro, *J. Am. Chem. Soc.* **1999**, *121*, 10632–10633; b) E. Sola, J. Navarro, J. A. López, F. J. Lahoz, L. A. Oro, H. Werner, *Organometallics* **1999**, *18*, 3534–3546; c) J. Navarro, M. Sagi, E. Sola, F. J. Lahoz, I. T. Dobrinovitch, A. Kathó, F. Joó, L. A. Oro, *Adv. Synth. Catal.* **2003**, *345*, 280–288.

[12] F. Torres, E. Sola, M. Martín, C. Ochs, G. Picazo, J. A. López, F. J. Lahoz, L. A. Oro, *Organometallics* **2001**, *20*, 2716–2724.

[13] P. Marcazzan, C. Abu-Gnim, K. N. Seneviratne, B. R. James, *Inorg. Chem.* **2004**, *43*, 4820–4824.

[14] A. Macchioni, *Chem. Rev.* **2005**, *105*, 2039–2073.

[15] P. Marcazzan, B. O. Patrick, B. R. James, *Organometallics* **2003**, *22*, 1177–1179.

[16] a) "3D Search and Research using the Cambridge Structural Database", F. H. Allen, O. Kennard, *Chem. Des. Automation News* **1993**, *8(1)*, 31; b) J. Dupont, C. S. Consorti, J. Spencer, *Chem. Rev.* **2005**, *105*, 2527–2571.

[17] a) P. Marcazzan, B. O. Patrick, B. R. James, *Organometallics* **2005**, *24*, 1445–1451; b) P. Marcazzan, B. O. Patrick, B. R. James, *Russ. Chem. Bull.* **2003**, *52*, 2715–2721; c) M. B. Ezhova, B. O. Patrick, B. R. James, *Organometallics* **2005**, *24*, 3753–3757.

[18] M. V. Jiménez, E. Sola, J. A. López, F. J. Lahoz, L. A. Oro, *Chem. Eur. J.* **1998**, *4*, 1398–1410.

[19] See, for example: E. Sola, V. I. Bakhmoutov, F. Torres, A. Elduque, J. A. López, F. J. Lahoz, H. Werner, L. A. Oro, *Organometallics* **1998**, *17*, 683–696.

[20] a) J. F. Lam, C. Yin, C. H. Yeung, S. M. Ng, G. Jia, C. P. Lau, *Organometallics* **2002**, *21*, 1898–1902; b) M. M. Abad, I. Atheaux, A. Maisonnat, B. Chaudret, *Chem. Commun.* **1999**, 381–382; c) A. Caballero, F. Jalón, B. Manzano, *Chem. Commun.* **1998**, 1879–1880; d) H. S. Chu, C. P. Lau, K. Y. Wong, W. T. Wong, *Organometallics* **1998**, *17*, 2768–2777; e) R. H. Crabtree, *Science* **1998**, *282*, 2000–2001; f) A. J. Lough, S. Park, R. Ramachandran, R. H. Morris, *J. Am. Chem. Soc.* **1994**, *116*, 8356–8357.

[21] K. A. Connors, *Chemical Kinetics, The Study of Reaction Rates in Solution*, VCH, Weinheim, **1990**, pp. 292–300.

[22] M. D. Fryzuk, P. A. MacNeil, S. J. Rettig, *J. Am. Chem. Soc.* **1987**, *109*, 2803–2812.

[23] a) A. Ienco, M. J. Calhorda, J. Reinhold, F. Reineri, C. Bianchini, M. Peruzzini, F. Vizza, C. Meali, *J. Am. Chem. Soc.* **2004**, *126*, 11954–11965; b) M. Pavlov, P. E. M. Siegbahn, M. R. A. Blomberg, R. H. Crabtree, *J. Am. Chem. Soc.* **1998**, *120*, 548–555.

[24] P. M. Morse, M. O. Spencer, S. R. Wilson, G. S. Girolami, *Organometallics* **1994**, *13*, 1646–1655.

[25] R. Usón, L. A. Oro, J. Cabeza, *Inorg. Synth.* **1985**, *23*, 126–130.

[26] R. H. Blessing, *Acta Crystallogr. Sect. A* **1995**, *51*, 33–38; SADABS: Area-detector absorption correction, **1996**, Bruker-AXS, Madison, WI.

[27] SHELXTL Package v. 6.10, Bruker-AXS, Madison, WI (USA), **2000**; G. M. Sheldrick, SHELXS-86 and SHELXL-97, University of Göttingen, Göttingen (Germany), **1997**.

[28] *TRC Thermodynamic Tables, Vol. VI*, p. K6170.

[29] Gaussian 98, Revision A.6, M. J. Frisch, G. W. Trucks, H. B. Schlegel, G. E. Scuseria, M. A. Robb, J. R. Cheeseman, V. G. Zakrzewski, J. A. Montgomery, R. E. Stratmann, J. C. Burant, S. Dapprich, J. M. Millam, A. D. Daniels, K. N. Kudin, M. C. Strain, O. Farkas, J. Tomasi, V. Barone, M. Cossi, R. Cammi, B. Mennucci, C. Pomelli, C. Adamo, S. Clifford, J. Ochterski, G. A. Petersson, P. Y. Ayala, Q. Cui, K. Morokuma, D. K. Malick, A. D. Rabuck, K. Raghavachari, J. B. Foresman, J. Cioslowski, J. V. Ortiz, A. G. Baboul, B. B. Stefanov, G. Liu, A. Liashenko, P. Piskorz, I. Komaromi, R. Gomperts, R. L. Martin, D. J. Fox, T. Keith, M. A. Al-Laham, C. Y. Peng, A. Nanayakkara, C. Gonzalez, M. Challacombe, P. M. W. Gill, B. G. Johnson, W. Chen, M. W. Wong, J. L. Andres, M. Head-Gordon, E. S. Replogle, J. A. Pople, Gaussian, Inc., Pittsburgh, PA, **1998**.

[30] a) S. Huzinaga, *J. Chem. Phys.* **1965**, *42*, 1293–1302; b) T. H. Dunning, *J. Chem. Phys.* **1970**, *53*, 2823–2833.

[31] P. J. Hay, W. R. Wadt, *J. Chem. Phys.* **1985**, *82*, 270–283.

[32] P. J. Hay, W. R. Wadt, *J. Chem. Phys.* **1985**, *82*, 284–298.

[33] P. J. Hay, W. R. Wadt, *J. Chem. Phys.* **1985**, *82*, 299–310.

[34] A. Höllwarth, M. Böhme, S. Dapprich, A. W. Ehlers, A. Gobbi, V. Jonas, K. F. Köhler, R. Stegmann, A. Veldkamp, G. Frenking, *Chem. Phys. Lett.* **1993**, *208*, 237–240.

[35] M. Couty, M. B. Hall, *J. Comput. Chem.* **1996**, *17*, 1359–1370.

[36] A. W. Ehlers, M. Böhme, S. Dapprich, A. Gobbi, A. Höllwarth, V. Jonas, K. F. Köhler, R. Stegmann, A. Veldkamp, G. Frenking, *Chem. Phys. Lett.* **1993**, *208*, 111–114.

Received: October 6, 2005
Published online: March 14, 2006

